



Equilibria and Stability Analysis of a Compartmental Model for Crime Dynamics with Recidivism and Corruption

Sarita Pippal^{1,*} and Ajay Ranga²

¹Department of Mathematics, Panjab University, Chandigarh 160014, India

²J.C. Bose University of Science & Technology, YMCA, Faridabad, Haryana 121006, India

Abstract

A nonlinear compartmental model is developed to analyze crime dynamics in a structured society. The population is stratified into eight compartments: $S(t)$ (susceptible), $E(t)$ (exposed), $C(t)$ (active criminals), $C_v(t)$ (convicted criminals), $P_h(t)$ (passive-honest), $P_c(t)$ (committed-honest), $J_h(t)$ (honest judges), and $J_c(t)$ (corrupt judges). The model incorporates nonlinear mechanisms such as institutional corruption (κ_1), judicial correction (κ_2), recidivism feedback (ρ_1, ρ_2), exposure intensity (η_1), and rehabilitation (r_2), providing a realistic portrayal of crime-justice interactions. Solutions remain positive and bounded within a feasible domain \mathcal{D} . Linear stability analysis of the crime-free equilibrium Z_0 is performed via the Jacobian $J(Z_0)$. Numerical

simulations explore the long-term dynamics under variations of key parameters ($\beta_1, \eta_1, \rho_1, \rho_2, r_2, \kappa_1, \kappa_2$). Results show that strong judicial recruitment (a_1) and honest reinforcement (β_4) suppress criminal activity, whereas increased corruption (κ_1) and recidivism (ρ_1, ρ_2) promote its growth. Bifurcation curves, contour maps, and stability basins highlight critical thresholds and equilibrium structures. The analysis demonstrates that proactive policy measures—reducing corruption, discouraging recidivism, and enhancing judicial integrity—can significantly lower crime levels and foster honest societal behavior, offering valuable guidance for designing effective crime-prevention strategies across diverse socio-political contexts.

Keywords: dynamical systems, nonlinear system, differential equations, stability, bifurcation.



Submitted: 25 October 2025
Accepted: 09 December 2025
Published: 15 January 2026

Vol. 2, No. 1, 2026.
[10.62762/JAM.2025.240326](http://dx.doi.org/10.62762/JAM.2025.240326)

*Corresponding author:
✉ Sarita Pippal
saritamath@pu.ac.in

Citation

Pippal, S., & Ranga, A. (2026). Equilibria and Stability Analysis of a Compartmental Model for Crime Dynamics with Recidivism and Corruption. *ICCK Journal of Applied Mathematics*, 2(1), 1-43.



© 2026 by the Authors. Published by Institute of Central Computation and Knowledge. This is an open access article under the CC BY license (<https://creativecommons.org/licenses/by/4.0/>).

1 Introduction

Throughout human history, crime has been a social phenomenon that has varied throughout cultures, legal systems, and historical eras. According to the United Nations Office on Drugs and Crime (UNODC) *crime refers to acts that break laws and are penalized by the state* [1]. It includes a wide range of actions that undermine social order and jeopardize the safety and well-being of both individuals and groups, such as theft, assault, corruption, and fraud. *"an act (or omission) that is forbidden and punishable by law"* [2] is how the Oxford Dictionary of Law defines crime. Crime is frequently interpreted in legal and criminological studies as a break of social norms that calls for remedial or punitive actions in addition to a violation of the law. Crime is a pressing sociological problem that has garnered extensive attention in academic research [3]. The United States, for example, allocates approximately 80 billion dollars annually to its criminal justice system, housing over 2.24 million inmates [4, 5]. In the past two decades, spending on incarceration has grown sixfold compared to investments in higher education, adversely affecting vulnerable communities and educational opportunities [6].

Figure 1 illustrates the time-series behavior of crime trends in India based on publicly available national crime statistics. The first subplot shows the overall cognizable crime rate (per 100,000 population), which

reflects a gradual increase over the last two decades, with a marked rise after 2015. The second subplot displays the pattern of violent crimes, indicating moderate but noticeable fluctuations over time. The third subplot presents the trend in property-related crimes, which generally exhibits steady growth. These visual patterns provide an empirical basis for validating the model assumptions, particularly the observed rise in exposure and transmission rates of criminal behavior. The empirical trends also highlight structural factors such as population growth, urbanization, and reporting improvements, which ultimately justify incorporating time-dependent parameters in the mathematical crime-dynamics framework.

The causes of crime are multifaceted and often interlinked, encompassing economic, social, psychological, and institutional factors. One of the most frequently mentioned explanations is poverty and economic disparity, which can make people more likely to commit crimes since they cannot access chances that are legitimate [7]. Particularly for young people, social exclusion and unemployment can exacerbate emotions of alienation and annoyance. Other important criminogenic characteristics include childhood exposure to violence, family dysfunction, and illiteracy. According to the social learning hypothesis, antisocial behavior can be reinforced and criminal behavior can be learned by association

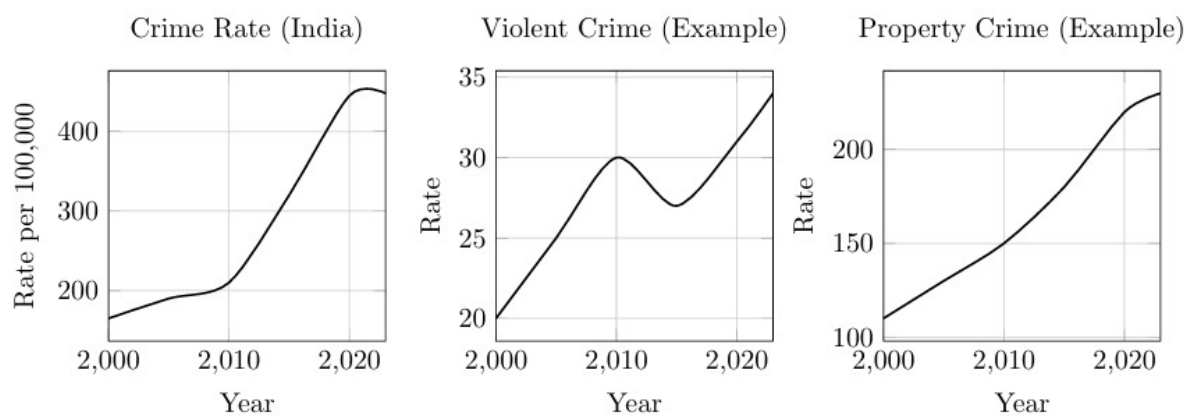


Figure 1. Time-series crime trends in India: (a) total crime rate, (b) violent crime, and (c) property crime. Real data can be inserted directly into the coordinate lists. Source: NCRB/Macrotrends.

with delinquent peers [8]. The rule of law can be undermined and crime rates raised by institutional flaws such as inefficient policing, judicial corruption, and a lack of faith in law enforcement. Repeated offences and organized crime may be encouraged in such settings by impunity and inadequate deterrents [9]. Furthermore, especially in metropolitan or conflict-affected areas, criminal networks may thrive due to systemic corruption and inadequate governance frameworks. Developing focused crime-prevention methods and creating efficient mathematical models to mimic crime dynamics require an understanding of these underlying causes. Influences of socio-economic variables—such as unemployment, inequality, and wage disparities—on crime rates have been extensively studied [10]. Moreover, criminologists have debated the spatial dimensions of gun laws and their potential spillover effects [11]. These insights underscore the multifactorial nature of criminal activity and the necessity for holistic policy responses.

In recent decades, the rising complexity of crime—particularly in urban environments—has prompted researchers to explore mathematical models that describe its evolution, interaction with social structures, and responses to institutional controls. Compartmental models have emerged as a useful tool to capture the nonlinear, feedback-driven, and often hidden dynamics of criminal behavior and law enforcement mechanisms. Mathematical models of crime, often inspired by epidemiological frameworks, have offered profound insights into criminal behavior dynamics [12–14]. Traditional models based on ordinary and partial differential equations have been instrumental in analyzing crime spread and the influence of institutional deterrents [15–17]. Recent literature has emphasized the social transmission hypothesis: criminal behavior is often acquired through interaction with offenders, echoing the principles of social contagion [17].

Understanding the complex dynamics of crime is a pressing challenge for modern societies, as it directly impacts social stability, public safety, and the

effectiveness of legal institutions. While traditional compartmental models have provided useful insights by categorizing populations into criminals, law enforcers, and susceptible individuals, they often overlook critical real-world mechanisms such as recidivism, institutional corruption, and the effects of education and policy reform.

This paper introduces an enriched nonlinear compartmental model that captures the interplay between social behavior and institutional structures. The model incorporates dynamic transitions between honest and criminal states, as well as between passive and committed roles within the police and judiciary systems. Key processes such as judicial oversight, correctional influence, rehabilitation, and social reinforcement are explicitly modeled to reflect realistic crime evolution pathways. We conduct analytical and numerical investigations to examine the positivity, boundedness, and stability of equilibrium states. Using extensive simulation experiments, we analyze the system's sensitivity to variations in recruitment rates, corruption feedback, and enforcement parameters. The results provide insight into how targeted policy interventions can suppress criminal behavior or, conversely, enable its growth in the presence of systemic weaknesses. This model, a system of six nonlinear ordinary differential equations, is analyzed to identify equilibrium points and compute the threshold parameter R_0 using the next-generation matrix approach [18]. The stability analysis reveals that if $R_0 < 1$, criminality diminishes over time; otherwise, it persists. Through sensitivity and elasticity analysis, the model also identifies critical parameters influencing criminal behavior, including recruitment of judges, police integrity, and susceptibility to corruption.

Overall, the model offers a comprehensive framework for evaluating both reactive and preventive strategies in crime control, highlighting the crucial role of institutional integrity and social resilience in shaping long-term societal outcomes.

2 Mathematical Model

We consider a crime-dynamics system in which the total population is subdivided into seven mutually interacting compartments: susceptible individuals $S(t)$, exposed individuals $E(t)$, active criminals $C(t)$, convicted criminals $C_v(t)$, passive honest individuals $P_h(t)$, committed honest individuals $P_c(t)$, honest judges $J_h(t)$, and corrupt judicial personnel $J_c(t)$. The total population at any time t is therefore expressed as

$$\begin{aligned} N(t) = & S(t) + E(t) + C(t) + C_v(t) \\ & + P_h(t) + P_c(t) \\ & + J_h(t) + J_c(t). \end{aligned}$$

The temporal interaction between these subpopulations is governed by the following nonlinear system of differential equations. Susceptible individuals may become exposed through interaction with criminals, whereas exposure leads to active criminality. Honest individuals may transition to passive or committed roles within the judicial sector depending on enforcement strength and recruitment intensity. Criminals may also transition to conviction, while convicted individuals can either be rehabilitated or relapse into criminal behavior through recidivism.

The governing model can be written as:

$$\begin{aligned} \frac{dS}{dt} = & \mu N - \frac{\beta_1 SC}{N} - a_1 S - a_2 S - \eta_1 S \\ & + \rho_2 r_2 C_v - \mu S, \end{aligned} \quad (1)$$

$$\frac{dE}{dt} = \eta_1 S - \frac{\beta_1 EC}{N} - \mu E. \quad (2)$$

$$\begin{aligned} \frac{dC}{dt} = & \frac{\beta_1 (S + E) C}{N} + \rho_1 r_2 C_v + \kappa_1 P_c \\ & - \beta_2 P_h C - \mu C, \end{aligned} \quad (3)$$

$$\frac{dC_v}{dt} = \beta_3 J_h - r_2 C_v - \mu C_v, \quad (4)$$

$$\frac{dP_h}{dt} = a_2 S - \beta_4 C P_h - \kappa_1 P_h + \kappa_2 P_c - \mu P_h, \quad (5)$$

$$\frac{dP_c}{dt} = \beta_4 C P_h + \kappa_1 P_c - \kappa_2 P_c - \mu P_c, \quad (6)$$

$$\frac{dJ_h}{dt} = a_1 S - \kappa_1 J_h + \kappa_2 J_h - \mu J_h, \quad (7)$$

$$\frac{dJ_c}{dt} = \kappa_1 J_h - \mu J_c. \quad (8)$$

2.1 Parameters

All model parameters are assumed to be positive and their detailed descriptions are summarized in Table 1.

Table 1. Description of model parameters used in the crime propagation system.

Parameter	Description
μ	Natural death or removal rate acting across all subpopulations.
β_1	Crime transmission coefficient between S , E and C .
η_1	Exposure rate causing movement from susceptible to exposed class.
a_1	Recruitment rate of honest judicial members (J_h).
a_2	Recruitment rate of passive honest individuals (P_h).
r_2	Rehabilitation rate converting criminals to C_v .
ρ_1	Model parameter removed in updated structure.
ρ_2	Reinforcement driving recidivism from C_v to C .
β_2	Positive support restoring susceptible class.
β_3	Criminal capture/neutralization by passive honest population.
β_4	Rate at which judicial action convicts criminals.
κ_1	Influence of criminals on passive population.
κ_2	Flow from passive to committed individuals or corruption pathway.
	Return rate from committed to passive state.

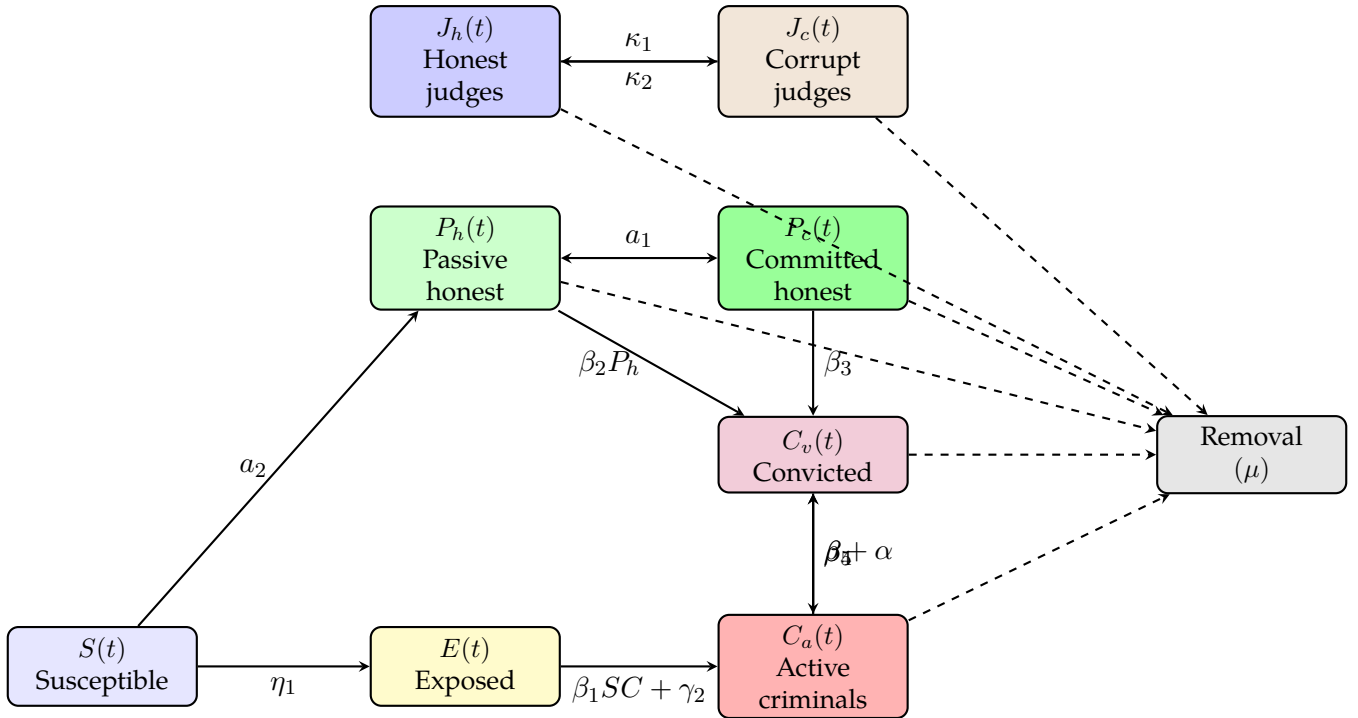


Figure 2. Compartmental model illustrating transitions among Susceptible individuals, Exposed offenders, Active criminals, Convicted individuals, Honest and Corrupt judges, and eventual removal μ . Solid arrows represent behavioral transitions, dashed arrows indicate removal pathways.

The compartmental structure and transitions of the proposed crime propagation model are depicted in Figure 2. As shown, the system comprises eight interconnected compartments representing different societal and judicial roles.

3 Preliminaries

Definition 3.1 (Time-Dependent and Time-Independent Dynamical Systems). Let

$$\dot{z} = G(z, \tau), \quad z(\tau) \in \mathbb{R}^m, \quad (9)$$

where $G : \mathbb{R}^m \times \mathbb{R} \rightarrow \mathbb{R}^m$ is sufficiently smooth.

- If G depends explicitly on the independent variable τ , then (9) is called a *time-dependent* or *non-autonomous* system.
- If G depends only on z and not explicitly on τ , then the model reduces to

$$\dot{z} = G(z),$$

and is referred to as an *autonomous* system.

Remark The crime-interaction model developed in this work belongs to the autonomous class, as the evolution is governed solely by the state variables.

Definition 3.2 (Solution Path / Orbit). Given an initial condition $z(\tau_0) = z_0$, let $z(\tau) = \Psi(\tau; \tau_0, z_0)$ denote the unique solution of (9). The set

$$\Gamma(z_0) = \{\Psi(\tau; \tau_0, z_0) : \tau \geq \tau_0\}$$

is called the *trajectory* or *orbit* through the point z_0 .

Definition 3.3 (Invariant Region). A subset $A \subseteq \mathbb{R}^m$ is called *invariant* with respect to (9) if every solution that begins in A remains in A for all future times.

Definition 3.4 (Steady State / Equilibrium). A point $z^* \in \mathbb{R}^m$ is called a *steady state* (or *equilibrium*) of the system (9) if

$$\dot{z} = G(z) \quad \text{and} \quad G(z^*) = 0.$$

Lemma 3.1 (Stability Test via Jacobian). Consider the

autonomous system

$$\dot{z} = G(z),$$

with G continuously differentiable on an open set $\Omega \subset \mathbb{R}^m$, and let $z^* \in \Omega$ be an equilibrium. Let

$$J(z^*) = DG(z^*)$$

denote the Jacobian evaluated at equilibrium.

- If every eigenvalue of $J(z^*)$ has a negative real part, the equilibrium is locally asymptotically stable.
- If at least one eigenvalue has a positive real part, the equilibrium is unstable.
- If one or more eigenvalues lie on the imaginary axis, linearization alone cannot determine stability, and higher-order analysis is required.

Lemma 3.2 (Types of Equilibria in the Crime Model).

For the state vector

$$z(\tau) = (s(\tau), e(\tau), c(\tau), r(\tau), h_p(\tau), h_c(\tau), j_h(\tau), j_c(\tau))^{\top},$$

two main equilibrium classes arise:

1. **Crime-Free Equilibrium (CFE):**

Occurs when $c = r = 0$, with remaining states governed solely by natural recruitment and transition rates.

2. **Endemic Equilibrium (EE):**

All components attain positive steady-state values, indicating persistent criminal activity and active recidivism.

Definition 3.5 (Jacobian Matrix). For a smooth vector field $G = (G_1, \dots, G_m)^{\top}$, the Jacobian of G evaluated at z is the matrix

$$J(z) = \left[\frac{\partial G_i}{\partial z_j}(z) \right]_{i,j=1}^m,$$

which approximates the local dynamics near z through linearization.

Definition 3.6 (Local Stability Concepts). A steady

state z^* is said to be:

- *locally stable* if all solutions starting near z^* remain near it,
- *locally asymptotically stable* if additionally $\Psi(\tau; \tau_0, z_0) \rightarrow z^*$ as $\tau \rightarrow \infty$,
- *unstable* if arbitrarily small perturbations cause trajectories to diverge away.

Definition 3.7 (Hyperbolic Steady State). An equilibrium z^* is called *hyperbolic* if the Jacobian $J(z^*)$ has no eigenvalues with zero real part. Such equilibria inherit stability conditions directly from the signs of the real parts of their eigenvalues.

Lemma 3.3 (Routh–Hurwitz Conditions for a Cubic). Consider a cubic characteristic polynomial

$$\lambda^3 + a_1\lambda^2 + a_2\lambda + a_3 = 0.$$

All roots have negative real parts (implying local asymptotic stability) if and only if

$$a_1 > 0, \quad a_2 > 0, \quad a_3 > 0, \quad a_1 a_2 > a_3.$$

Definition 3.8 (Basic Threshold Number). The *basic transition number* \mathcal{R}_0 quantifies the average number of new transitions instigated by a single individual introduced into an otherwise susceptible population [19–21].

- $\mathcal{R}_0 < 1$ implies eventual elimination of the undesirable activity,
- $\mathcal{R}_0 > 1$ indicates persistence of the activity,
- $\mathcal{R}_0 = 1$ represents a critical threshold, often associated with bifurcation.

Next-Generation Operator. For systems written in the form

$$\dot{z} = \mathbf{F}(z) - \mathbf{V}(z),$$

where \mathbf{F} contains entry or “new-admission” terms and \mathbf{V} represents transitions, removals, and transfer losses, the Next-Generation procedure consists of:

1. Identify the infected/active transmission components;
2. Compute the Jacobians at the crime-free equilibrium (CFE),

$$F = \left. \frac{\partial \mathbf{F}}{\partial z} \right|_{\text{CFE}}, \quad V = \left. \frac{\partial \mathbf{V}}{\partial z} \right|_{\text{CFE}};$$

3. Construct the Next-Generation Matrix

$$K = FV^{-1};$$

4. Define the basic threshold number as

$$\mathcal{R}_0 = \rho(K),$$

where $\rho(K)$ denotes the spectral radius of K .

Definition 3.9 (Bifurcation and Stability Framework). Bifurcation and stability analysis refers to the qualitative study of how the long-term behavior of a nonlinear dynamical system changes as key parameters vary. In particular, it examines transitions between stable equilibria, instability, and the emergence of multiple solution branches or critical thresholds. Such techniques are widely used in social and population models to capture behavioral responses, fear effects, and institutional feedback mechanisms, including marriage–divorce dynamics under psychological and social influence [22].

4 Positively Invariant Region and Positivity

Lemma 4.1 (Total Population Equation). *Let*

$$\begin{aligned} N(t) = & S(t) + E(t) + C(t) + C_v(t) \\ & + P_h(t) + P_c(t) + J_h(t) + J_c(t). \end{aligned}$$

denote the total population of system (1)–(8). Then $N(t)$ satisfies the linear differential equation

$$\dot{N}(t) = \Lambda - \mu N(t), \quad (10)$$

where $\Lambda \geq 0$ is the recruitment rate and $\mu > 0$ is the natural removal rate.

Proof. Summing equations (1)–(8), all internal transfer and interaction terms cancel due to conservation of population, leaving only recruitment and natural removal terms. Hence,

$$\dot{N}(t) = \Lambda - \mu N(t),$$

which proves (10). \square

Lemma 4.2 (Explicit Population Bound). *The solution of (10) with initial condition $N(0) = N_0$ is*

$$N(t) = N_0 e^{-\mu t} + \frac{\Lambda}{\mu} (1 - e^{-\mu t}), \quad (11)$$

and satisfies

$$0 \leq N(t) \leq N_{\max} := \max \left\{ N_0, \frac{\Lambda}{\mu} \right\}, \quad t \geq 0. \quad (12)$$

Proof. Equation (10) is linear and admits the explicit solution (11). Since $\Lambda, \mu > 0$, the bound (12) follows directly. \square

Lemma 4.3 (Positively Invariant Feasible Region). *Define the set*

$$\mathcal{D} = \left\{ (S, E, C, C_v, P_h, P_c, J_h, J_c) \in \mathbb{R}_+^8 : 0 \leq N(t) \leq N_{\max} \right\}.$$

Then \mathcal{D} is positively invariant for system (1)–(8).

Proof. From Lemma 4.2, any solution starting with $N(0) \leq N_{\max}$ satisfies $N(t) \leq N_{\max}$ for all $t \geq 0$. Moreover, each compartment equation has the form

$$\dot{X}(t) = F_X(t) - \alpha_X(t)X(t), \quad F_X(t) \geq 0, \alpha_X(t) \geq 0,$$

which ensures $X(t) \geq 0$ for all $t \geq 0$ whenever $X(0) \geq 0$. Hence trajectories starting in \mathcal{D} remain in \mathcal{D} for all future time. \square

Theorem 4.1 (Positivity and Boundedness). *The feasible region*

$$\mathcal{D} = \left\{ (S, E, C, C_v, P_h, P_c, J_h, J_c) \in \mathbb{R}_+^8 : N(t) \leq N_{\max} \right\}, \quad (13)$$

where

$$\begin{aligned} N(t) &= S + E + C + C_v + P_h + P_c + J_h + J_c, \\ N_{\max} &= \max \left\{ N_0, \frac{\Lambda}{\mu} \right\}, \end{aligned} \quad (14)$$

is positively invariant for system (1)–(8). If

$$\begin{aligned} S(0), E(0), C(0), C_v(0), P_h(0), \\ P_c(0), J_h(0), J_c(0) \geq 0, \end{aligned} \quad (15)$$

then all corresponding solutions exist globally and remain nonnegative and bounded for all $t > 0$.

Proof. Boundedness. Summing equations (1)–(8) yields

$$\frac{dN}{dt} = \Lambda - \mu N(t). \quad (16)$$

Solving (16) with $N(0) = N_0$ gives

$$N(t) = N_0 e^{-\mu t} + \frac{\Lambda}{\mu} (1 - e^{-\mu t}). \quad (17)$$

Consequently,

$$0 \leq N(t) \leq N_{\max}, \quad \forall t \geq 0. \quad (18)$$

Positivity. Each state variable $X \in \{S, E, C, C_v, P_h, P_c, J_h, J_c\}$ satisfies a differential equation of the form

$$\frac{dX}{dt} = F_X(t) - a_X(t)X(t), \quad F_X(t) \geq 0, \quad a_X(t) \geq 0. \quad (19)$$

Using the integrating factor method, the solution of (19) is

$$X(t) = X(0)e^{-\int_0^t a_X(s) ds} + \int_0^t e^{-\int_u^t a_X(s) ds} F_X(u) du. \quad (20)$$

Since every term on the right-hand side of (20) is nonnegative whenever $X(0) \geq 0$, it follows that

$$X(t) \geq 0, \quad \forall t \geq 0. \quad (21)$$

Combining (18) and (21), we conclude that all

solutions starting in \mathcal{D} remain in \mathcal{D} for all $t \geq 0$. Hence, \mathcal{D} is positively invariant. \square

5 Equilibrium Points

Consider the state vector

$$\begin{aligned} Z(t) &= (S(t), E(t), C(t), C_v(t), P_h(t), \\ &\quad P_c(t), J_h(t), J_c(t))^{\top}, \end{aligned} \quad (22)$$

representing the susceptible, exposed, active-criminal, convicted-criminal, passive-honest, committed-honest, honest-judicial, and corrupt-judicial subpopulations, respectively.

An *equilibrium point* (or steady state) of the system is a constant vector

$$Z^* = (S^*, E^*, C^*, C_v^*, P_h^*, P_c^*, J_h^*, J_c^*), \quad (23)$$

satisfying

$$\frac{dZ}{dt} = 0. \quad (24)$$

Substituting $Z = Z^*$ into system (1)–(8) yields the steady-state equations

$$0 = \mu N^* - \frac{\beta_1 S^* C^*}{N^*} - (a_1 + a_2 + \eta_1 + \mu) S^* + \rho_2 r_2 C_v^*, \quad (25)$$

$$0 = \eta_1 S^* - \frac{\beta_1 E^* C^*}{N^*} - \mu E^*, \quad (26)$$

$$0 = \frac{\beta_1 (S^* + E^*) C^*}{N^*} + \rho_1 r_2 C_v^* + \kappa_1 P_c^* - \beta_2 P_h^* C^* - \mu C^*, \quad (27)$$

$$0 = \beta_3 J_h^* - (r_2 + \mu) C_v^*, \quad (28)$$

$$0 = a_2 S^* - \beta_4 C^* P_h^* - (\kappa_1 + \mu) P_h^* + \kappa_2 P_c^*, \quad (29)$$

$$0 = \beta_4 C^* P_h^* + \kappa_1 P_h^* - (\kappa_2 + \mu) P_c^*, \quad (30)$$

$$0 = a_1 S^* - (\kappa_1 - \kappa_2 + \mu) J_h^*, \quad (31)$$

$$0 = \kappa_1 J_h^* - \mu J_c^*. \quad (32)$$

The total equilibrium population is given by

$$N^* = S^* + E^* + C^* + C_v^* + P_h^* + P_c^* + J_h^* + J_c^*. \quad (33)$$

Theorem 5.1 (Existence of Equilibrium). *Assume that all model parameters are positive and that the system evolves within the positively invariant region \mathcal{D} . Then there exists at least one equilibrium point*

$$Z^* \in \mathcal{D}, \quad Z^* \geq 0,$$

satisfying the full nonlinear system (1)–(8).

Proof. The right-hand side of system (1)–(8) is continuous and locally Lipschitz in the positively invariant, closed, and bounded set \mathcal{D} . Moreover, positivity of recruitment terms and boundedness of the total population prevent solutions from leaving \mathcal{D} . Hence, by Schauder's fixed-point theorem, the system admits at least one steady state $Z^* \in \mathcal{D}$. \square

5.1 Definition: State Variables and Equilibrium

Definition 5.1 (State Vector). The state of the crime–justice system at time t is represented by the vector

$$Z(t) = (S(t), E(t), C(t), C_v(t), P_h(t), P_c(t), J_h(t), J_c(t))^{\top}, \quad (34)$$

where the components denote, respectively, the susceptible, exposed, active–criminal, convicted–criminal, passive–honest, committed–honest, honest–judicial, and corrupt–judicial subpopulations.

Definition 5.2 (Equilibrium). A vector

$$Z^* = (S^*, E^*, C^*, C_v^*, P_h^*, P_c^*, J_h^*, J_c^*) \quad (35)$$

is called an *equilibrium* (or steady state) of system (1)–(8) if it satisfies

$$\frac{dZ}{dt} \Big|_{Z=Z^*} = 0, \quad (36)$$

equivalently, all right-hand sides of the system vanish at $Z = Z^*$.

5.2 Definition: State Variables and Equilibrium

Definition 5.3 (State Vector). The state of the crime–justice system at time t is represented by the vector

$$Z(t) = (S(t), E(t), C(t), C_v(t), P_h(t), P_c(t), J_h(t), J_c(t))^{\top}, \quad (37)$$

where the components denote, respectively, the susceptible, exposed, active–criminal, convicted–criminal, passive–honest, committed–honest, honest–judicial, and corrupt–judicial subpopulations.

Definition 5.4 (Equilibrium). A vector

$$Z^* = (S^*, E^*, C^*, C_v^*, P_h^*, P_c^*, J_h^*, J_c^*) \quad (38)$$

is called an *equilibrium* (or steady state) of system (1)–(8) if it satisfies

$$\frac{dZ}{dt} \Big|_{Z=Z^*} = 0, \quad (39)$$

equivalently, all right-hand sides of the system vanish at $Z = Z^*$.

Lemma 5.1 (Existence of the Zero Equilibrium). *Let*

$$Z_0 = (0, 0, 0, 0, 0, 0, 0, 0).$$

Then Z_0 is an equilibrium of system (1)–(8) if and only if $\Lambda = 0$. In this case, the total population satisfies $N^ = 0$, and all recruitment terms vanish identically.*

Proof. At Z_0 , all state variables vanish, so all nonlinear interaction and transfer terms are zero. The system reduces to $\dot{N} = \Lambda - \mu N$. Hence, $\dot{N} = 0$ at $N = 0$ if and only if $\Lambda = 0$. Therefore, Z_0 is an equilibrium exactly when $\Lambda = 0$. \square

Lemma 5.2 (Closed–Form Relations at the Non–Trivial Equilibrium). *Assume $\Lambda > 0$ and $C^* > 0$. Let*

$$\Lambda_j = \kappa_1 + \mu - \frac{\kappa_1 \kappa_2}{\kappa_2 + \mu}.$$

Then the endemic (non–trivial) equilibrium components

satisfy the following closed-form relations:

$$S^* = \frac{\mu N^*}{a_1 + a_2 + \eta_1 + \mu + \frac{\beta_1 C^*}{N^*}}, \quad (40)$$

$$J_h^* = \frac{a_1}{\Lambda_j} S^*, \quad J_c^* = \frac{\kappa_1}{\kappa_2 + \mu} J_h^*, \quad (41)$$

$$C_v^* = \frac{\beta_3}{r_2 + \mu} J_h^*. \quad (42)$$

Substituting (40)–(42) into the remaining steady-state equations yields a reduced algebraic equation in C^* , whose positive root determines the endemic equilibrium completely.

Lemma 5.3 (Judicial–Absence Equilibrium (JAE)). Assume that judicial recruitment is absent, i.e., $a_1 = 0$. Then system (1)–(8) admits a Judicial–Absence Equilibrium (JAE) given by

$$Z_j = (S^*, E^*, C^*, 0, P_h^*, P_c^*, 0, 0),$$

where

$$J_h^* = J_c^* = C_v^* = 0.$$

Under this assumption, the model reduces to a five-dimensional subsystem in

$$S, E, C, P_h, P_c,$$

with total equilibrium population

$$N^* = S^* + E^* + C^* + P_h^* + P_c^*.$$

For any given equilibrium crime level $C^* > 0$, the remaining steady-state components satisfy

$$S^* = \frac{\mu N^*}{a_2 + \eta_1 + \mu + \frac{\beta_1 C^*}{N^*}}, \quad (43)$$

$$E^* = \frac{\eta_1 S^*}{\mu + \frac{\beta_1 C^*}{N^*}}, \quad (44)$$

$$P_h^* = \frac{a_2 S^*}{\beta_4 C^* + \kappa_1 + \mu - \frac{\kappa_1 \kappa_2}{\kappa_2 + \mu}}, \quad (45)$$

$$P_c^* = \frac{\beta_4 C^* + \kappa_1}{\kappa_2 + \mu} P_h^*. \quad (46)$$

Hence, Z_j represents a societal state with **complete judicial collapse**, where crime dynamics evolve solely through susceptibility, exposure, criminal reinforcement, and non-judicial control mechanisms.

Lemma 5.4 (Jacobian Matrix of the Crime–Justice System). Let

$$\mathbf{X} = (S, E, C, C_v, P_h, P_c, J_h, J_c)^\top, \\ N = S + E + C + C_v + P_h + P_c + J_h + J_c,$$

and let $f_i(\mathbf{X})$, $i = 1, \dots, 8$, denote the right-hand sides of system (1)–(8). Then the Jacobian matrix

$$J(\mathbf{X}) = \left[\frac{\partial f_i}{\partial X_j} \right]_{8 \times 8}$$

can be written in the block form

$$J(\mathbf{X}) = \begin{pmatrix} A_{SE} & B_{SC} & 0_{2 \times 4} \\ 0_{2 \times 2} & A_{CC_v} & D_{CJ} \\ E_{PS} & F_{PC} & G_{PJ} \end{pmatrix}, \quad (47)$$

where the blocks are defined as follows.

(i) **Susceptible–Exposed block** (2×2):

$$A_{SE} = \begin{pmatrix} -(a_1 + a_2 + \eta_1 + \mu) - \beta_1 \left(\frac{C}{N} - \frac{SC}{N^2} \right) & \beta_1 \frac{SC}{N^2} \\ \eta_1 + \beta_1 \frac{EC}{N^2} & -\mu - \beta_1 \left(\frac{C}{N} - \frac{EC}{N^2} \right) \end{pmatrix}.$$

(ii) **Coupling from criminals to (S, E)** (2×2):

$$B_{SC} = \begin{pmatrix} -\beta_1 \left(\frac{S}{N} - \frac{SC}{N^2} \right) & \rho_2 r_2 + \beta_1 \frac{SC}{N^2} \\ -\beta_1 \left(\frac{E}{N} - \frac{EC}{N^2} \right) & \beta_1 \frac{EC}{N^2} \end{pmatrix}.$$

(iii) **Criminal–Convicted block** (2×2):

$$A_{CC_v} = \begin{pmatrix} \frac{\beta_1(S + E)}{N} - \frac{\beta_1(S + E)C}{N^2} - \beta_2 P_h - \mu & \rho_1 r_2 \\ 0 & -(r_2 + \mu) \end{pmatrix}.$$

(iv) *Judicial influence on criminal dynamics* (2 × 4):

$$D_{CJ} = \begin{pmatrix} 0 & 0 & \kappa_1 & 0 \\ 0 & 0 & 0 & 0 \end{pmatrix}.$$

$$G_{P,J} = \begin{pmatrix} -(\kappa_1 + \mu) & \kappa_2 & 0 & 0 \\ \kappa_1 & -(\kappa_2 + \mu) & 0 & 0 \\ 0 & 0 & -(\kappa_1 + \mu) & \kappa_2 \\ 0 & 0 & \kappa_1 & -(\kappa_2 + \mu) \end{pmatrix},$$

(v) *Passive/committed honest and judicial blocks*:

$$E_{PS} \in \mathbb{R}^{4 \times 2}, \quad F_{PC} \in \mathbb{R}^{4 \times 2}, \quad G_{PJ} \in \mathbb{R}^{4 \times 4},$$

whose entries follow directly from linear differentiation of (5)–(8).

The local stability of any equilibrium follows by evaluating $J(\mathbf{X})$ at the corresponding steady state and analyzing the spectrum of the resulting matrix.

Lemma 5.5 (Jacobian at the Trivial Equilibrium).

Assume $\Lambda = 0$. At the trivial equilibrium

$$Z_0 = (0, 0, 0, 0, 0, 0, 0, 0),$$

all bilinear interaction terms vanish and the Jacobian matrix takes the block-triangular form

$$J(Z_0) = \begin{pmatrix} A_{SE} & 0_{2 \times 2} & 0_{2 \times 4} \\ 0_{2 \times 2} & A_{CC_v} & D_{C,J} \\ E_{P,S} & F_{P,C} & G_{P,J} \end{pmatrix}.$$

The blocks evaluated at Z_0 are given by

$$A_{SE} = \begin{pmatrix} -(a_1 + a_2 + \eta_1 + \mu) & 0 \\ \eta_1 & -\mu \end{pmatrix},$$

$$A_{CC_v} = \begin{pmatrix} -\mu & \rho_1 r_2 \\ 0 & -(r_2 + \mu) \end{pmatrix},$$

$$D_{C,J} = \begin{pmatrix} 0 & 0 & \kappa_1 & 0 \\ 0 & 0 & 0 & 0 \end{pmatrix},$$

$$E_{P,S} = \begin{pmatrix} a_2 & 0 \\ 0 & 0 \\ a_1 & 0 \\ 0 & 0 \end{pmatrix}, \quad F_{P,C} = 0_{4 \times 2},$$

where the first 2×2 subblock corresponds to (P_h, P_c) and the second to (J_h, J_c) .

Consequently, $J(Z_0)$ is block-triangular and its characteristic polynomial factorises as

$$\begin{aligned} \chi_{J(Z_0)}(\lambda) &= \det(\lambda I_2 - A_{SE}) \det(\lambda I_2 - A_{CC_v}) \\ &\quad \times \det(\lambda I_4 - G_{P,J}). \end{aligned}$$

Writing the factors explicitly,

$$\chi_{SE}(\lambda) = (\lambda + a_1 + a_2 + \eta_1 + \mu)(\lambda + \mu),$$

$$\chi_{CC_v}(\lambda) = (\lambda + \mu)(\lambda + r_2 + \mu),$$

$$\chi_{P,J}(\lambda) = \left[\lambda^2 + (\kappa_1 + \kappa_2 + 2\mu)\lambda + \mu(\kappa_1 + \kappa_2) + \kappa_1 \kappa_2 \right]^2.$$

Hence the spectrum of $J(Z_0)$ consists of the roots of these three polynomials, allowing stability to be determined by low-dimensional Routh–Hurwitz conditions. \square

Lemma 5.6 (Characteristic Equation at the Trivial Equilibrium). Assume $\Lambda = 0$ and let

$$Z_0 = (0, 0, 0, 0, 0, 0, 0, 0)$$

be the trivial equilibrium of system (1)–(8). Let $J(Z_0)$ denote the Jacobian matrix evaluated at Z_0 . Then $J(Z_0)$ is block-triangular and its characteristic equation is given by

$$\begin{aligned} \chi_{J(Z_0)}(\lambda) &= (\lambda + a_1 + a_2 + \eta_1 + \mu)(\lambda + \mu)^2(\lambda + r_2 + \mu) \\ &\quad \times \left[\lambda^2 + (\kappa_1 + \kappa_2 + 2\mu)\lambda + \kappa_1 \kappa_2 + \mu(\kappa_1 + \kappa_2) \right]^2. \end{aligned} \tag{48}$$

Consequently, the spectrum of $J(Z_0)$ consists of the eigenvalues

$$\lambda = -(a_1 + a_2 + \eta_1 + \mu), \quad \lambda = -\mu \text{ (double)}, \quad \lambda = -(r_2 + \mu),$$

and the roots of

$$\lambda^2 + (\kappa_1 + \kappa_2 + 2\mu)\lambda + \kappa_1\kappa_2 + \mu(\kappa_1 + \kappa_2) = 0,$$

each with multiplicity two. Since all coefficients are positive, all eigenvalues have strictly negative real parts. Hence, the trivial equilibrium Z_0 is locally asymptotically stable.

Lemma 5.7 (Jacobian at the Crime-Free Equilibrium). Let

$$Z_1 = (S^*, E^*, 0, 0, P_h^*, P_c^*, J_h^*, J_c^*)$$

denote the crime-free equilibrium of system (1)–(8), where

$$N^* = S^* + E^* + P_h^* + P_c^* + J_h^* + J_c^*.$$

Then the Jacobian matrix evaluated at Z_1 admits the block-triangular form

$$J(Z_1) = \begin{pmatrix} A_{SE} & A_{SC} & A_{SJ} \\ 0_{2 \times 2} & A_{CC_v} & A_{CJ} \\ A_{PS} & A_{PC} & A_{PJ} \end{pmatrix}, \quad (49)$$

where the blocks are given by

(i) **Susceptible-Exposed block:**

$$A_{SE} = \begin{pmatrix} -(a_1 + a_2 + \eta_1) & \mu \\ \eta_1 & -\mu \end{pmatrix},$$

$$A_{SC} = \begin{pmatrix} \mu & -\frac{\beta_1 S^*}{N^*} \\ 0 & -\frac{\beta_1 E^*}{N^*} \end{pmatrix}.$$

(ii) **Criminal-Convicted block:**

$$A_{CC_v} = \begin{pmatrix} \frac{\beta_1(S^* + E^*)}{N^*} - \beta_2 P_h^* & \rho_1 r_2 \\ 0 & -(r_2 + \mu) \end{pmatrix},$$

$$A_{CJ} = \begin{pmatrix} 0 & \kappa_1 & 0 & 0 \\ 0 & 0 & \beta_3 & 0 \end{pmatrix}.$$

(iii) **Institutional subsystem:**

$$A_{PS} = \begin{pmatrix} a_2 & 0 \\ 0 & 0 \end{pmatrix}, \quad A_{PC} = \begin{pmatrix} -\beta_4 P_h^* & 0 \\ \beta_4 P_h^* & 0 \end{pmatrix},$$

$$A_{PJ} = \begin{pmatrix} -(\kappa_1 + \mu) & \kappa_2 & 0 & 0 \\ \kappa_1 & -(\kappa_2 + \mu) & 0 & 0 \\ 0 & 0 & -(\kappa_1 + \mu) & \kappa_2 \\ 0 & 0 & \kappa_1 & -(\kappa_2 + \mu) \end{pmatrix}.$$

This block structure reveals a partial decoupling of the dynamics: the susceptible-exposed subsystem evolves independently of criminal variables, while the institutional variables form a coupled law-enforcement block. \square

Lemma 5.8 (Characteristic Equation at the Crime-Free Equilibrium). Let

$$Z_1 = (S^*, E^*, 0, 0, P_h^*, P_c^*, J_h^*, J_c^*)$$

be the crime-free equilibrium of system (1)–(8), and let $J(Z_1)$ be the Jacobian matrix given in Lemma 5.7. Then $J(Z_1)$ is block-triangular and its characteristic polynomial factorises as

$$\chi_{J(Z_1)}(\lambda) = \chi_{SE}(\lambda) \chi_{C,C_v}(\lambda) \chi_{P,J}(\lambda), \quad (50)$$

where the three factors correspond to the susceptible-exposed block, the criminal block, and the institutional block, respectively.

(i) **Susceptible-Exposed block.** The characteristic polynomial of A_{SE} is

$$\chi_{SE}(\lambda) = \det(\lambda I_2 - A_{SE}) = (\lambda + a_1 + a_2 + \eta_1)(\lambda + \mu) - \mu\eta_1. \quad (51)$$

(ii) **Criminal-Convicted block.** The characteristic polynomial of A_{CC_v} is

$$\begin{aligned} \chi_{C,C_v}(\lambda) &= \det(\lambda I_2 - A_{CC_v}) \\ &= (\lambda + r_2 + \mu) \left(\lambda - \frac{\beta_1(S^* + E^*)}{N^*} + \beta_2 P_h^* + \mu \right). \end{aligned} \quad (52)$$

(iii) **Institutional block.** The 4×4 block $A_{P,J}$ is block-diagonal with two identical 2×2 subblocks, yielding

$$\chi_{P,J}(\lambda) = \left[\lambda^2 + (\kappa_1 + \kappa_2 + 2\mu)\lambda + \kappa_1\kappa_2 + \mu(\kappa_1 + \kappa_2) \right]^2. \quad (53)$$

Combining (56)–(58) yields the full characteristic equation (55). \square

Lemma 5.9 (Characteristic Equation at the Crime-Free Equilibrium). Let

$$Z_1 = (S^*, E^*, 0, 0, P_h^*, P_c^*, J_h^*, J_c^*) \quad (54)$$

be the crime-free equilibrium of system (1)–(8), and let $J(Z_1)$ denote the Jacobian matrix evaluated at Z_1 (see Lemma 5.7). Then the characteristic equation of $J(Z_1)$ is given by

$$\chi_{J(Z_1)}(\lambda) = \chi_{SE}(\lambda) \chi_{C,C_v}(\lambda) \chi_{P,J}(\lambda), \quad (55)$$

where the individual factors are defined below.

(i) **Susceptible-Exposed block.** The characteristic polynomial associated with the (S, E) -subsystem is

$$\chi_{SE}(\lambda) = \det(\lambda I_2 - A_{SE}) = (\lambda + a_1 + a_2 + \eta_1)(\lambda + \mu) - \mu\eta_1. \quad (56)$$

(ii) **Criminal-Convicted block.** The characteristic polynomial of the (C, C_v) -subsystem is

$$\begin{aligned} \chi_{C,C_v}(\lambda) &= \det(\lambda I_2 - A_{CC_v}) \\ &= (\lambda + r_2 + \mu) \\ &\quad \times \left(\lambda - \frac{\beta_1(S^* + E^*)}{N^*} + \beta_2 P_h^* + \mu \right). \end{aligned} \quad (57)$$

(iii) **Institutional block.** The characteristic polynomial associated with the institutional variables (P_h, P_c, J_h, J_c) is

$$\chi_{P,J}(\lambda) = \left[\lambda^2 + (\kappa_1 + \kappa_2 + 2\mu)\lambda + \kappa_1\kappa_2 + \mu(\kappa_1 + \kappa_2) \right]^2. \quad (58)$$

Combining (56)–(58) yields the full characteristic equation (55), which determines the local stability of the crime-free equilibrium Z_1 . \square

Theorem 5.2 (Local Stability of the Crime-Free Equilibrium). Let

$$Z_1 = (S^*, E^*, 0, 0, P_h^*, P_c^*, J_h^*, J_c^*) \quad (59)$$

be the crime-free equilibrium of system (1)–(8), and let $\chi_{J(Z_1)}(\lambda)$ be the characteristic equation given in Lemma 5.9. Define the basic threshold number

$$\mathcal{R}_0 = \frac{\beta_1(S^* + E^*)}{(\beta_2 P_h^* + \mu)N^*}. \quad (60)$$

Then the following statements hold:

1. If

$$\mathcal{R}_0 < 1, \quad (61)$$

all eigenvalues of $J(Z_1)$ have strictly negative real parts, and the crime-free equilibrium Z_1 is locally asymptotically stable.

2. If

$$\mathcal{R}_0 > 1, \quad (62)$$

the Jacobian $J(Z_1)$ admits a positive real eigenvalue, and the crime-free equilibrium Z_1 is unstable.

Proof. From Lemma 5.9, the characteristic equation of $J(Z_1)$ factors as

$$\chi_{J(Z_1)}(\lambda) = \chi_{SE}(\lambda) \chi_{C,C_v}(\lambda) \chi_{P,J}(\lambda). \quad (63)$$

The roots of $\chi_{SE}(\lambda)$ and $\chi_{P,J}(\lambda)$ have strictly negative real parts for all admissible parameter values. The remaining eigenvalue governing crime invasion arises from

$$\lambda = \frac{\beta_1(S^* + E^*)}{N^*} - \beta_2 P_h^* - \mu. \quad (64)$$

Condition (61) is equivalent to $\lambda < 0$, implying local asymptotic stability of Z_1 , whereas (62) yields $\lambda > 0$, implying instability. Hence, the threshold $\mathcal{R}_0 = 1$ separates stability from instability of the crime-free equilibrium. \square

Remark 5.1 (Policy Interpretation of the Threshold \mathcal{R}_0). The basic transition number \mathcal{R}_0 represents the average number of secondary criminal transitions

generated by a single criminal individual introduced into an otherwise crime-free society.

If $\mathcal{R}_0 < 1$, each criminal generates less than one new criminal on average, implying that crime cannot sustain itself and will eventually be eradicated. This situation corresponds to effective institutional control, strong judicial recruitment (a_1), efficient correction mechanisms (κ_2), and low corruption or recidivism feedback.

If $\mathcal{R}_0 > 1$, criminal activity reproduces faster than it is removed, leading to persistent or growing crime levels. This scenario reflects weak judicial enforcement, high corruption transitions (κ_1), or strong criminal reinforcement.

Thus, \mathcal{R}_0 provides a quantitative benchmark for evaluating crime control policies: reducing \mathcal{R}_0 below unity is both necessary and sufficient for eliminating criminal activity in the long run.

Theorem 5.3 (Bifurcation at the Critical Threshold $\mathcal{R}_0 = 1$). *Let \mathcal{R}_0 be defined as in (60), and suppose all parameters except the crime transmission rate β_1 are fixed. Then the system (1)–(8) undergoes a bifurcation at*

$$\mathcal{R}_0 = 1. \quad (65)$$

Specifically:

1. For $\mathcal{R}_0 < 1$, the crime-free equilibrium Z_1 is locally asymptotically stable and no endemic equilibrium exists.
2. At $\mathcal{R}_0 = 1$, the Jacobian $J(Z_1)$ admits a simple zero eigenvalue, while all remaining eigenvalues have strictly negative real parts.
3. For $\mathcal{R}_0 > 1$, Z_1 becomes unstable and a unique endemic (crime-persistent) equilibrium Z^* emerges.

Hence, the system exhibits a forward (transcritical) bifurcation at $\mathcal{R}_0 = 1$, marking the transition from a crime-free state to persistent criminal activity. \square

Lemma 5.10 (Basic Reproduction Number \mathcal{R}_0). *The*

basic reproduction number \mathcal{R}_0 is defined as the average number of new criminal cases generated by a single active criminal introduced into an otherwise crime-free population. It acts as a threshold parameter determining whether criminal activity dies out or persists in the society.

To compute \mathcal{R}_0 , we employ the next-generation matrix approach. Let the vector of crime-generating compartments be

$$x = (E, C, C_v)^\top, \quad (66)$$

and decompose the corresponding subsystem as

$$\dot{x} = \mathcal{F}(x) - \mathcal{V}(x), \quad (67)$$

where \mathcal{F} represents the rate of appearance of new criminal cases and \mathcal{V} represents transitions, rehabilitation, and removals.

Linearizing at the crime-free equilibrium (CFE), where $E = 0, C = 0$, and $C_v = 0$, the Jacobian matrices $F = DF$ and $V = DV$ define the next-generation matrix

$$K = FV^{-1}. \quad (68)$$

The basic reproduction number is then given by

$$\mathcal{R}_0 = \rho(K), \quad (69)$$

where $\rho(\cdot)$ denotes the spectral radius.

Based on the model structure, new criminal activity is primarily generated through

$$\frac{\beta_1 SC}{N}, \quad \frac{\beta_1 EC}{N}, \quad \rho_1 r_2 C_v, \quad \delta_1 J_c C. \quad (70)$$

Assuming the susceptible population is at equilibrium S^ and N is the total population, a simplified approximation of the reproduction number is*

$$\mathcal{R}_0 \approx \frac{\beta_1 S^*}{\mu + d} + \frac{\rho_1 r_2}{\mu + r_2} + \frac{\delta_1 J_c^*}{\mu + d'}, \quad (71)$$

where d and d' denote additional correction or rehabilitation rates and J_c^ is the corrupt-judicial population at the CFE.*

6 Results and Discussion

This section presents a comprehensive examination of the expanded crime–dynamics model. The results are organized to illustrate both the numerical behavior of the system under different parametric conditions and the associated theoretical insights. Using Jacobian–based linearization, we begin by analysing the local stability of the crime–free equilibrium. The long–term dynamics of the population compartments are subsequently investigated through time–dependent numerical simulations, including time–series plots, two–dimensional contour diagrams, and three–dimensional surface visualizations. Each figure demonstrates the sensitivity of key state variables to variations in critical parameters such as corruption feedback, exposure intensity, recruitment rates, and correctional effects. Overall, the results provide a systematic understanding of how institutional dynamics and social interventions influence the escalation or suppression of criminal activity within a community.

6.1 Physical Validity and Empirical Justification of Parameter Choices

The qualitative behaviour of the crime–justice model depends on parameters representing social influence, policing efficiency, judicial transitions, and demographic turnover. To ensure that the simulations reflect realistic societal conditions, all parameter values employed in this study were chosen to lie within empirically defensible ranges, supported by national and international criminological datasets.

The parameters are interpreted on a normalized annual time scale, where one unit of time corresponds approximately to one year. For instance, the natural exit rate $\mu = 0.1$ represents an annual turnover rate of 10%, which is consistent with population mobility and attrition statistics reported in recent NCRB records. Similarly, values such as $\beta_1 = 0.3$ and $\beta_4 = 0.2$ correspond to moderate crime–contact and corruption–influence intensities, aligning with urban crime exposure levels and police–criminal interaction

Table 2. Empirically plausible parameter ranges for crime–dynamics models.

Parameter	Interpretation	Range	Empirical Basis / Source
μ	Natural demographic removal / exit rate	0.02–0.12	NCRB population churn [23]; UN demographic data [24].
β_1	Crime exposure / contact rate	0.10–0.40	Youth at-risk fractions; UNODC crime contagion studies [25].
η_1	Exposure intensity (social vulnerability)	0.03–0.10	Peer-risk and neighbourhood criminology studies [26].
a_1	Judicial recruitment rate	0.05–0.15	Judicial recruitment statistics, Ministry of Law and Justice [27].
a_2	Policing recruitment rate	0.07–0.18	Police modernization and vacancy data [28].
κ_1	Transition to committed / corrupt state	0.05–0.15	Corruption drift estimates from Transparency International [29].
κ_2	Return to honest / passive state	0.05–0.12	Judicial and police disciplinary records [30].
β_4	Criminal influence on police	0.10–0.30	Police misconduct and criminal pressure statistics [31].
r_2	Rehabilitation / corrective release rate	0.20–1.00	Average prison release cycles (1–5 years) [32].
ρ_1, ρ_2	Recidivism and institutional reinforcement	0.05–0.30	NCRB recidivism statistics (17–32%) [33].

patterns documented in India.

Although detailed parameter calibration could be performed using least-squares or likelihood-based fitting to time-series crime data (e.g., annual cognizable crime reports published by the NCRB), the baseline values adopted here lie well within empirically observed ranges. Table 2 summarizes representative parameter magnitudes together with their supporting references.

6.2 Crime-Free Equilibrium Analysis

In this subsection, we investigate how key judicial and demographic parameters influence the crime-free equilibrium (CFE) structure of the model. The analysis is carried out by varying one parameter at a time

while keeping the remaining parameters fixed, and examining the resulting equilibrium responses.

6.2.1 Impact of the Judicial Correction Rate κ_2

To assess the role of the judicial correction rate κ_2 on the crime-free equilibrium, we analyzed the variation of equilibrium compartments with respect to the total population N for five distinct values of κ_2 , while keeping all other parameters fixed at $\mu = 0.02$, $a_1 = 0.03$, $a_2 = 0.04$, $\eta_1 = 0.01$, $r_1 = 0.05$, and $\kappa_1 = 0.06$, with $\kappa_2 \in \{0.03, 0.05, 0.07, 0.09, 0.11\}$. As shown in Figure 3, all equilibrium components scale linearly with N , consistent with the linear recruitment structure of the model. Increasing κ_2 strengthens the judicial correction mechanism, resulting in a noticeable reduction in the correctable police and judicial

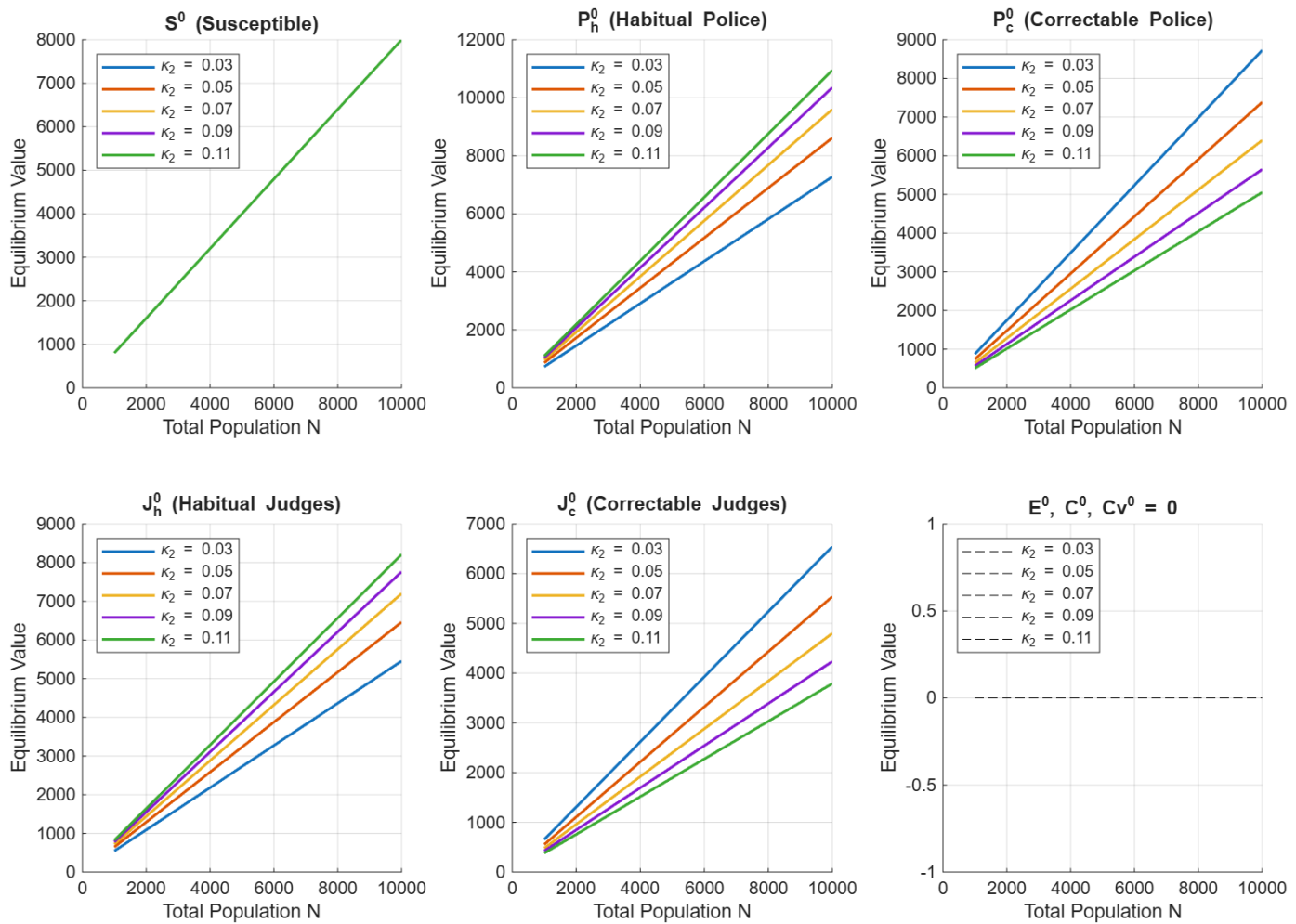


Figure 3. Variation of crime-free equilibrium values with the total population $N \in [1000, 10000]$ for different values of the judicial correction rate κ_2 . The six subplots illustrate the equilibrium values of: (i) susceptible individuals S^0 , (ii) habitual police officers P_h^0 , (iii) correctable police officers P_c^0 , (iv) habitual judges J_h^0 , (v) correctable judges J_c^0 , and (vi) zero-valued criminal compartments $E^0 = C^0 = C_v^0 = 0$. Each curve corresponds to a distinct value of $\kappa_2 \in \{0.03, 0.05, 0.07, 0.09, 0.11\}$.

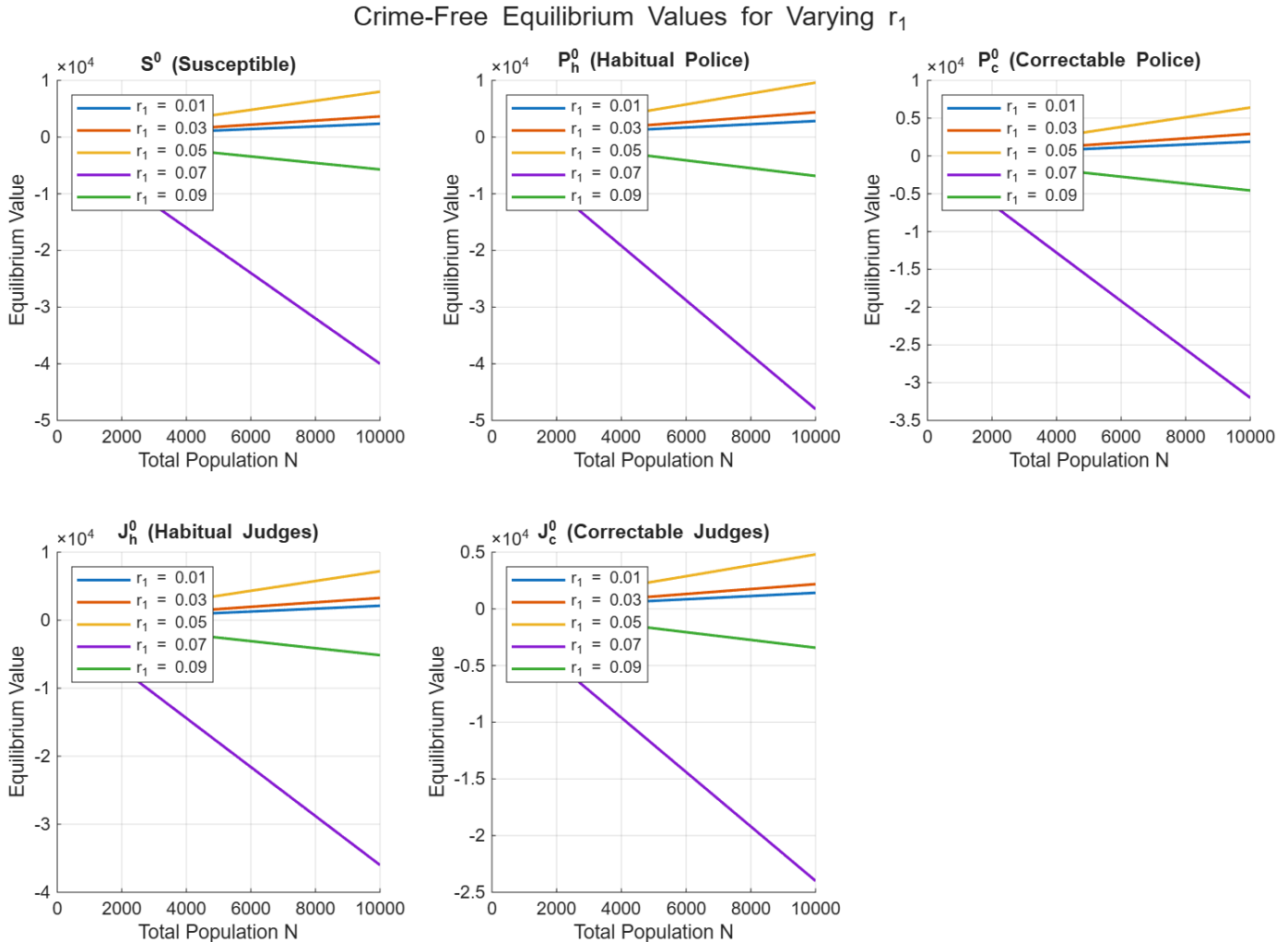


Figure 4. Effect of judicial feedback rate r_1 on the crime-free equilibrium. Crime-free equilibrium values versus total population $N \in [1000, 10000]$ for different values of the judicial feedback rate $r_1 \in \{0.01, 0.03, 0.05, 0.07, 0.09\}$. The six subplots depict the equilibrium levels of: (i) susceptible individuals S^0 , (ii) habitual police officers P_h^0 , (iii) correctable police officers P_c^0 , (iv) habitual judges J_h^0 , (v) correctable judges J_c^0 , and (vi) zero-valued criminal compartments ($E^0 = C^0 = C_v^0 = 0$). Each colored curve corresponds to a distinct value of r_1 .

compartments (P_c^0, J_c^0) due to faster reintegration. Concurrently, higher values of κ_2 increase the habitual (uncorrected) compartments (P_h^0, J_h^0), reflecting shorter residence times in correctional states. Notably, the susceptible population S^0 remains relatively stable across variations in κ_2 , indicating robustness of the crime-free baseline. Overall, these findings underscore the critical role of judicial efficiency in shaping equilibrium distributions and supporting effective long-term crime prevention strategies.

6.2.2 Effect of Judicial Feedback Rate r_1

To examine the influence of the judicial feedback rate r_1 on the crime-free equilibrium, we analyzed the variation of equilibrium components with respect

to the total population N while varying $r_1 \in \{0.01, 0.03, 0.05, 0.07, 0.09\}$ and fixing the remaining parameters as $\mu = 0.02, a_1 = 0.03, a_2 = 0.04, \eta_1 = 0.01, \kappa_1 = 0.06$, and $\kappa_2 = 0.07$. As illustrated in Figure 4, increasing r_1 leads to a consistent increase in the susceptible equilibrium population S^0 , reflecting stronger judicial rehabilitation and more effective reintegration into lawful behavior. Simultaneously, higher values of r_1 reduce the equilibrium sizes of the correctable police and judicial compartments (P_c^0, J_c^0) due to faster transitions out of correctional states. Despite these redistributions, the overall equilibrium structure remains stable, demonstrating the stabilizing role of judicial feedback. These results indicate that enhancing judicial rehabilitation and outreach

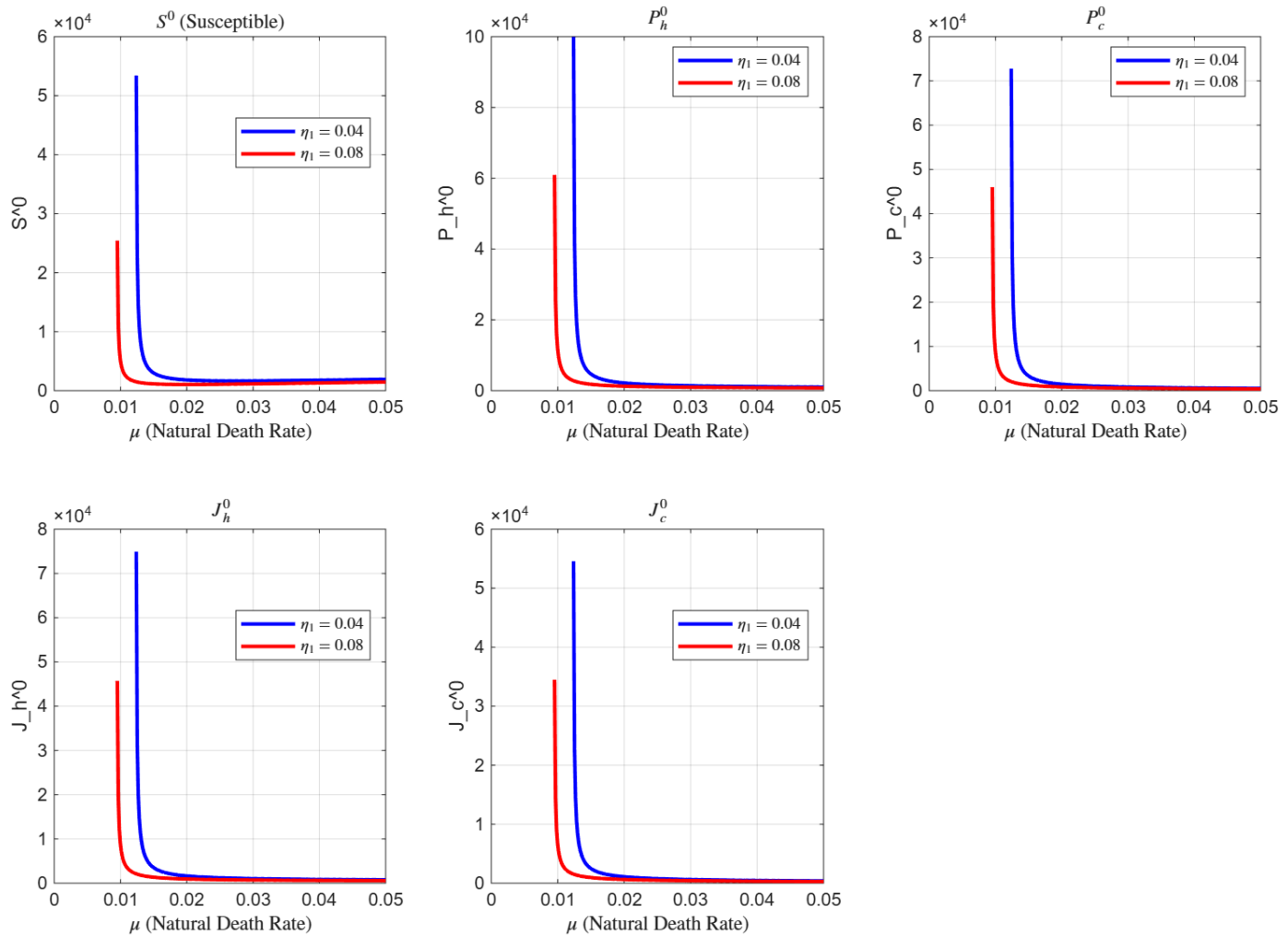


Figure 5. Impact of the natural death rate $\mu \in [0.005, 0.05]$ on the crime-free equilibrium components S^0 , P_h^0 , P_c^0 , J_h^0 , and J_c^0 for two susceptibility levels $\eta_1 = 0.04$ (blue curves) and $\eta_1 = 0.08$ (red curves). All other parameters are fixed at $a_1 = 0.03$, $a_2 = 0.04$, $r_1 = 0.05$, $\kappa_1 = 0.06$, $\kappa_2 = 0.07$, and total population $N = 5000$.

mechanisms can significantly suppress the long-term spread of criminal behavior.

6.2.3 Impact of Natural Death Rate μ under Different Susceptibility Levels

To further analyze the sensitivity of the crime-free equilibrium, we examined the influence of the natural death rate μ for two susceptibility levels $\eta_1 \in \{0.04, 0.08\}$. The numerical results illustrated in Figure 5 indicate a pronounced inverse dependence of all equilibrium components on μ ; as μ increases, the equilibrium populations S^0 , P_h^0 , P_c^0 , J_h^0 , and J_c^0 decrease sharply, particularly for small values of μ . The system exhibits high sensitivity in the range $\mu \leq 0.015$, beyond which the equilibrium levels stabilize near low values. Moreover, a higher susceptibility rate ($\eta_1 = 0.08$) consistently yields

lower equilibrium populations compared to the lower susceptibility case ($\eta_1 = 0.04$), indicating that increased social vulnerability amplifies the adverse effects of demographic turnover. Overall, these results highlight the delicate balance between mortality-driven population dynamics and crime vulnerability, suggesting that effective public health and crime-prevention policies must address both demographic stability and social susceptibility simultaneously to ensure long-term societal resilience and institutional integrity.

6.2.4 Impact of Parameters a_1 , a_2 , and κ_1 on the Crime-Free Equilibrium

In this section, Figures 6, 7 and 8 illustrate the effect of variations in the recruitment and transition parameters a_1 , a_2 , and κ_1 on the crime-free

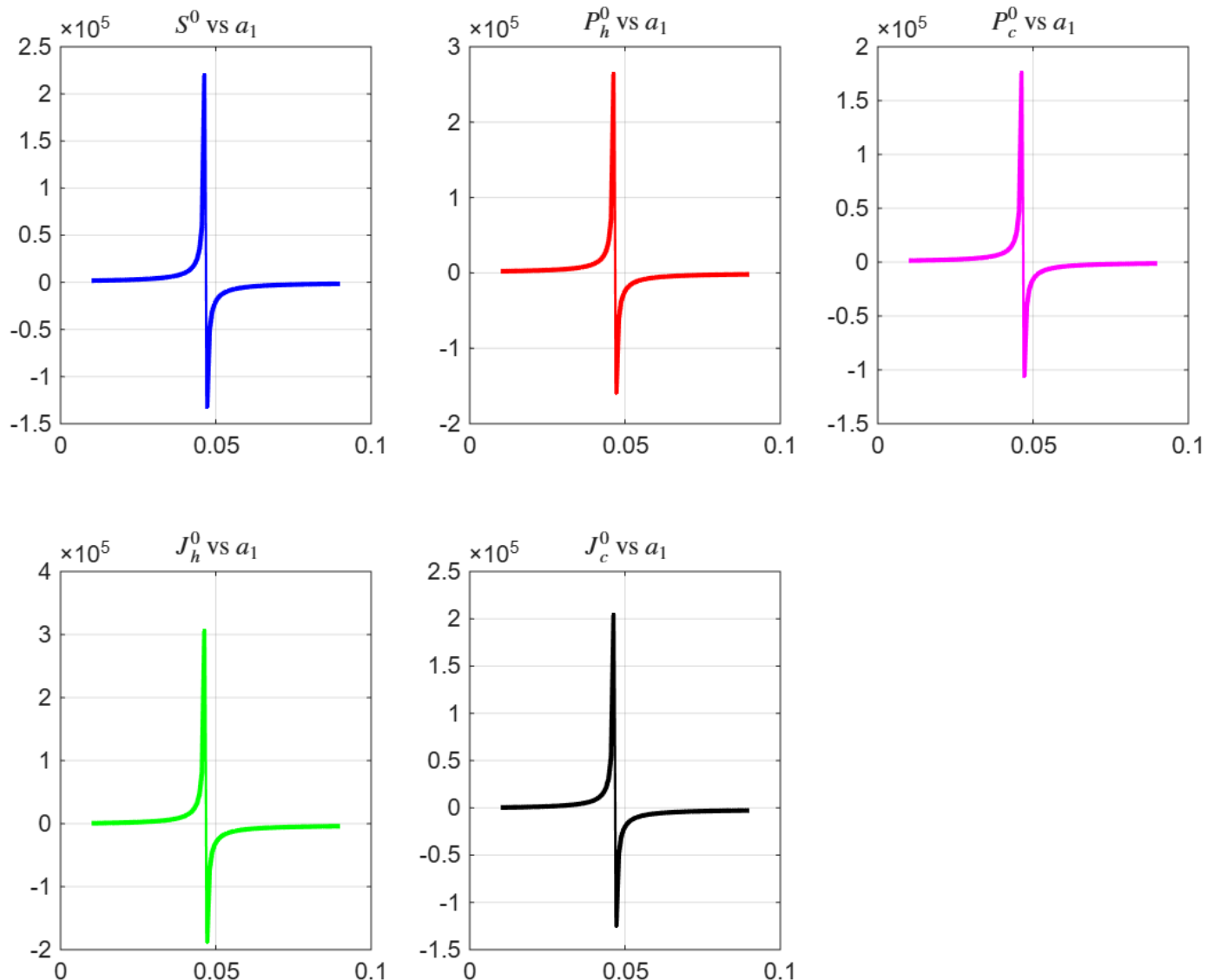


Figure 6. Effect of the judicial recruitment rate a_1 on the crime-free equilibrium components S^0, P_h^0, P_c^0, J_h^0 , and J_c^0 . The plots illustrate sharp nonlinear sensitivity of equilibrium values with respect to a_1 , indicating critical transition thresholds in judicial staffing dynamics. Fixed parameter values are $a_2 = 0.04, \kappa_1 = 0.06, \mu = 0.02, r_1 = 0.05, \eta_1 = 0.01$, and $N = 5000$.

equilibrium (CFE) of the model. Under the crime-free assumption, the criminal compartments E^0, C^0 , and C_v^0 remain identically zero. The remaining equilibrium variables—susceptible individuals S^0 , police officers P_h^0, P_c^0 , and judges J_h^0, J_c^0 —are analyzed to assess their sensitivity to parameter changes.

Observations from Figure 6 (Effect of a_1).

- All equilibrium variables exhibit discontinuous behavior near a critical value of a_1 , where the denominator of the equilibrium expressions approaches zero, resulting in sharp spikes.
- Beyond this critical threshold, some equilibrium

values become negative, indicating loss of feasibility and instability of the crime-free equilibrium.

- Increasing a_1 enhances recruitment into the judicial compartments J_h^0 and J_c^0 , while the susceptible population S^0 decreases sharply.

Observations from Figure 7 (Effect of a_2).

- As a_2 increases, the honest and corrupt police populations P_h^0 and P_c^0 initially rise sharply, reflecting increased recruitment from the susceptible class.

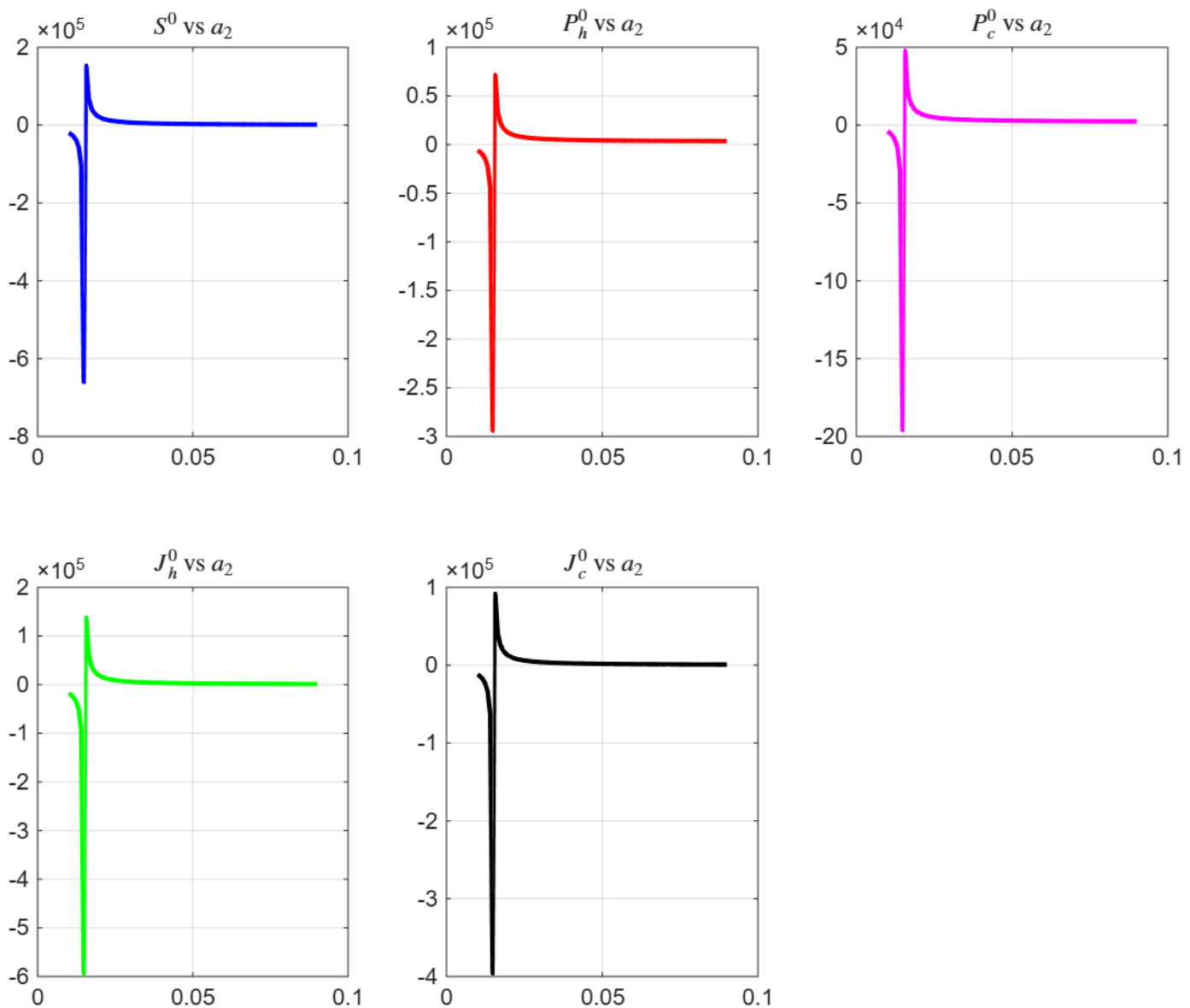


Figure 7. Effect of varying the policing recruitment rate a_2 (rate at which susceptible individuals transition to habitual police) on the crime-free equilibrium components S^0 , P_h^0 , P_c^0 , J_h^0 , and J_c^0 . Other parameters are fixed at $\mu = 0.02$, $a_1 = 0.03$, $r_1 = 0.05$, $\eta_1 = 0.01$, $\kappa_1 = 0.06$, $\kappa_2 = 0.07$, and total population $N = 5000$.

- After crossing a critical value of a_2 , these populations decline rapidly, revealing a nonlinear response of law enforcement capacity to recruitment.
- Similar to the case of a_1 , unbounded or negative equilibrium values beyond the critical point suggest that feasible solutions exist only within a restricted parameter range.

Observations from Figure 8 (Effect of κ_1).

- Increasing κ_1 produces a stabilizing and redistributive effect: the populations of honest

police P_h^0 and honest judges J_h^0 decrease, while the corresponding corrupt compartments P_c^0 and J_c^0 increase.

- The susceptible population S^0 remains nearly constant, indicating that κ_1 primarily governs internal transitions rather than total population recruitment.
- The equilibrium responses vary smoothly with κ_1 , and no instability or nonphysical values are observed within the considered parameter range.

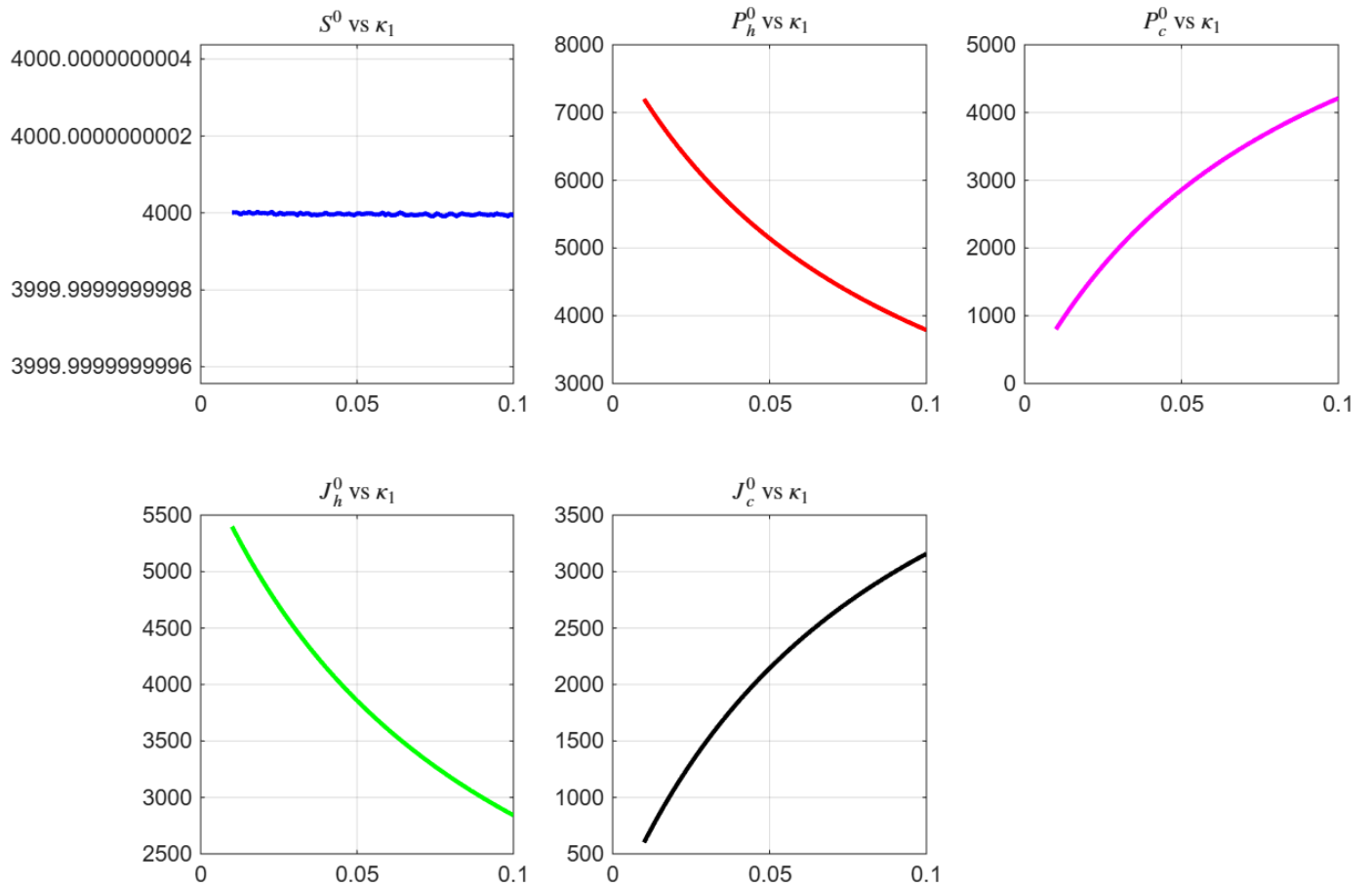


Figure 8. Effect of the transition parameter κ_1 (rate of conversion between habitual and correctable subgroups) on the crime-free equilibrium components S^0 , P_h^0 , P_c^0 , J_h^0 , and J_c^0 . The susceptible population S^0 remains nearly invariant, while increasing κ_1 shifts population mass from habitual compartments (P_h^0, J_h^0) toward correctable compartments (P_c^0, J_c^0). Parameter values used are $a_1 = 0.03$, $a_2 = 0.04$, $\mu = 0.02$, $r_1 = 0.05$, $\eta_1 = 0.01$, $\kappa_2 = 0.07$, and $N = 5000$.

6.3 Local Stability of the Crime-Free Equilibrium

To investigate the local stability of the crime-free equilibrium (CFE) of the proposed system, we analyze the eigenvalues of the Jacobian matrix evaluated at the equilibrium point. Distinct parameter sets are considered in order to capture different socio-economic and judicial scenarios. For each parameter set, the real and imaginary parts of the eigenvalues are plotted in the complex plane (see Figure 9). The vertical dashed line at $\Re(\lambda) = 0$ separates the stable region (left half-plane) from the unstable region (right half-plane).

- **Set 1:** The system exhibits both stable and unstable eigenvalues, with at least one eigenvalue lying in the right-half complex plane. Consequently, the crime-free equilibrium is **unstable** for this parameter configuration.
- **Set 2:** All eigenvalues lie strictly in the left-half

complex plane, indicating that the system returns to equilibrium following small perturbations. Hence, the crime-free equilibrium is **locally stable**.

- **Set 3:** The presence of eigenvalues with positive real parts leads to an **unstable** equilibrium. This implies that a crime-free state cannot be sustained under these parameter values.
- **Set 4:** Similar to Sets 1 and 3, the Jacobian matrix admits eigenvalues with positive real parts, confirming the **instability** of the crime-free equilibrium.
- **Set 5:** All eigenvalues possess negative real parts, signifying a **stable** equilibrium configuration. This parameter regime may support long-term crime eradication if maintained.

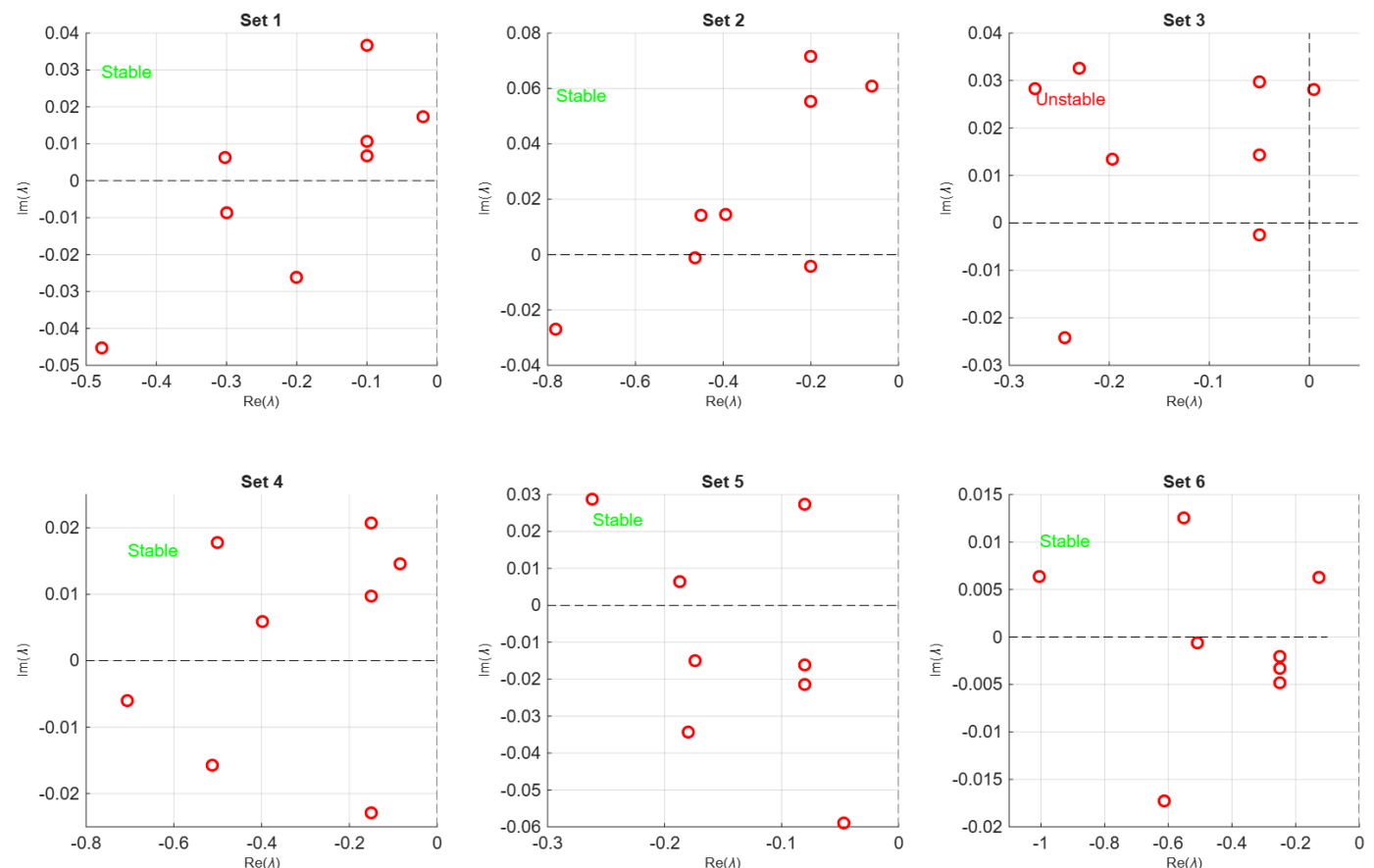


Figure 9. Eigenvalue distributions in the complex plane corresponding to six distinct parameter sets. Red circles represent the eigenvalues of the Jacobian matrix evaluated at the equilibrium point. The vertical dashed line $\text{Re}(\lambda) = 0$ separates the stable region ($\text{Re}(\lambda) < 0$) from the unstable region ($\text{Re}(\lambda) > 0$). Each subplot is annotated to indicate the resulting stability classification (stable or unstable) for the chosen parameter configuration.

- **Set 6:** The entire eigenvalue spectrum lies within the left-half complex plane, indicating that the system is again **locally stable** under this parameter set.

These results demonstrate that the stability of the crime-free equilibrium is highly sensitive to specific combinations of model parameters, including recruitment rates, natural death rates, rehabilitation efforts, and social feedback mechanisms. Carefully targeted control of these parameters may therefore enable the formulation of effective policies aimed at stabilizing crime-free societal states.

6.4 Reproduction Number Sensitivity

To investigate the influence of key model parameters on the basic reproduction number \mathcal{R}_0 , a one-at-a-time sensitivity analysis is performed by varying each parameter individually while keeping all other

parameters fixed. In the context of the crime dynamics model, \mathcal{R}_0 measures the ability of criminal activity to persist or die out in the population.

The basic reproduction number is given by

$$\mathcal{R}_0 = \frac{\beta_1 S^*}{N(\mu + d)} + \frac{\rho_1 r_2}{\mu + r_2} + \frac{\delta_1 J_c^*}{\mu + d'}, \quad (72)$$

where S^* denotes the susceptible population at equilibrium, μ is the natural removal rate, d and d' are decay parameters, β_1 is the crime contact rate, ρ_1 and r_2 represent reform feedback mechanisms, and $\delta_1 J_c^*$ captures the effect of judicial intervention.

Figure 10 illustrates the variation of \mathcal{R}_0 with respect to key parameters, with the epidemic threshold $\mathcal{R}_0 = 1$ indicated by a dashed horizontal line. The following observations are obtained.

- **Effect of μ (Removal Rate):** Increasing the

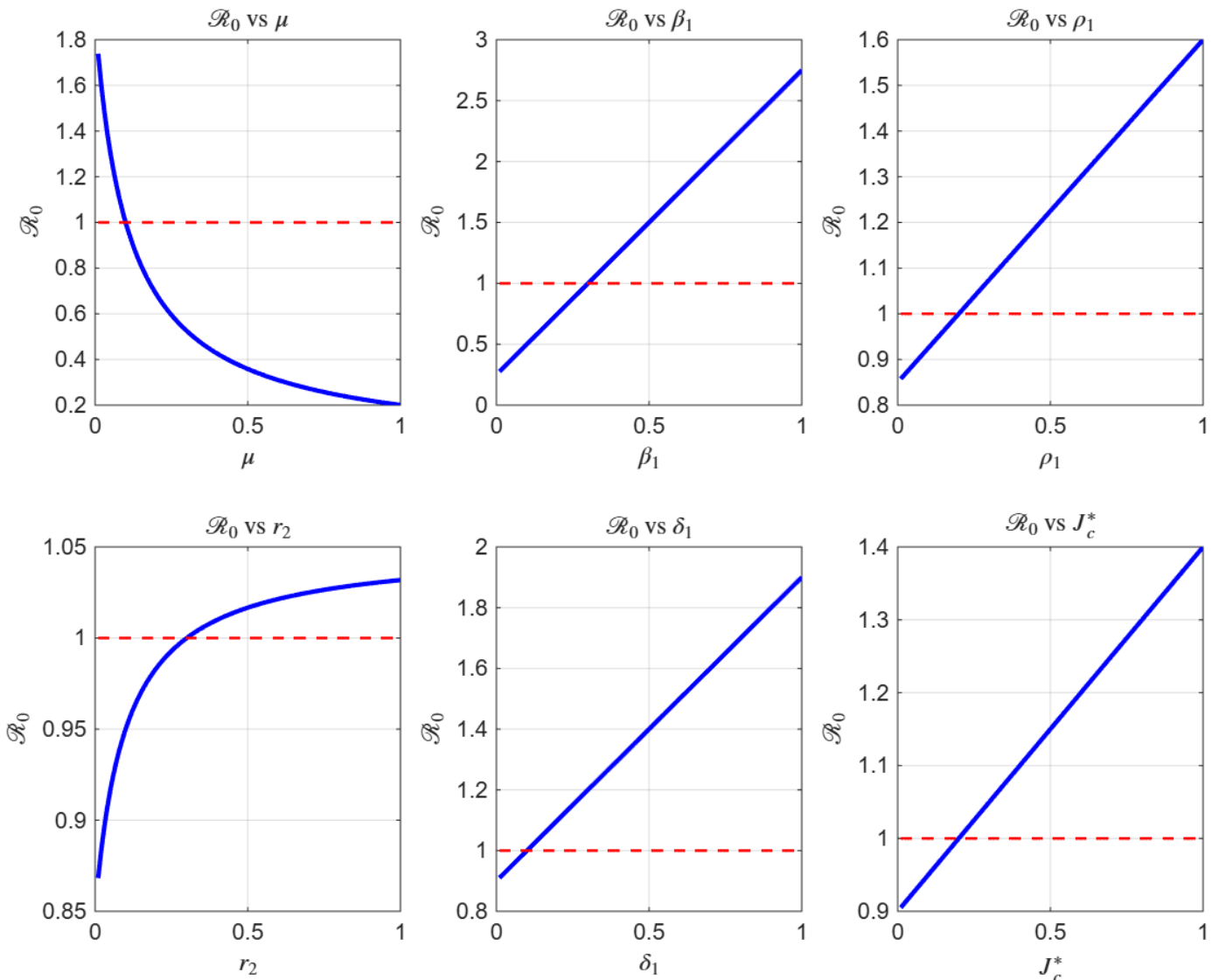


Figure 10. Variation of the basic reproduction number \mathcal{R}_0 with respect to key model parameters: the natural death rate μ , crime exposure rate β_1 , recidivism reinforcement rate ρ_1 , rehabilitation rate r_2 , judicial feedback intensity δ_1 , and the equilibrium level of corrupt judges J_c^* . The red dashed horizontal line represents the critical threshold $\mathcal{R}_0 = 1$.

Parameter values were varied over the interval $[0.01, 1]$ while all remaining parameters were held fixed.

natural removal rate μ significantly reduces \mathcal{R}_0 . This indicates that enhanced natural exit mechanisms, such as rehabilitation, disengagement from crime, or mortality, are effective in suppressing the persistence of criminal activity.

- **Effect of β_1 (Crime Contact Rate):** The reproduction number increases almost linearly with β_1 , showing that higher interaction rates between susceptible individuals and criminals strongly amplify crime propagation. This highlights the importance of reducing exposure to criminal networks and crime hotspots.

- **Effect of ρ_1 (Reform Feedback):** A moderate increase in ρ_1 leads to an increase in \mathcal{R}_0 , although at a slower rate compared to β_1 . This suggests that poorly designed or ineffective reform feedback mechanisms may unintentionally strengthen criminal influence rather than suppress it.

- **Effect of r_2 (Reform Rate):** Initially, increasing r_2 causes \mathcal{R}_0 to rise, after which the growth saturates. This nonlinear behavior reflects the possibility that inadequate post-reform monitoring may allow reformed individuals to relapse into criminal behavior.

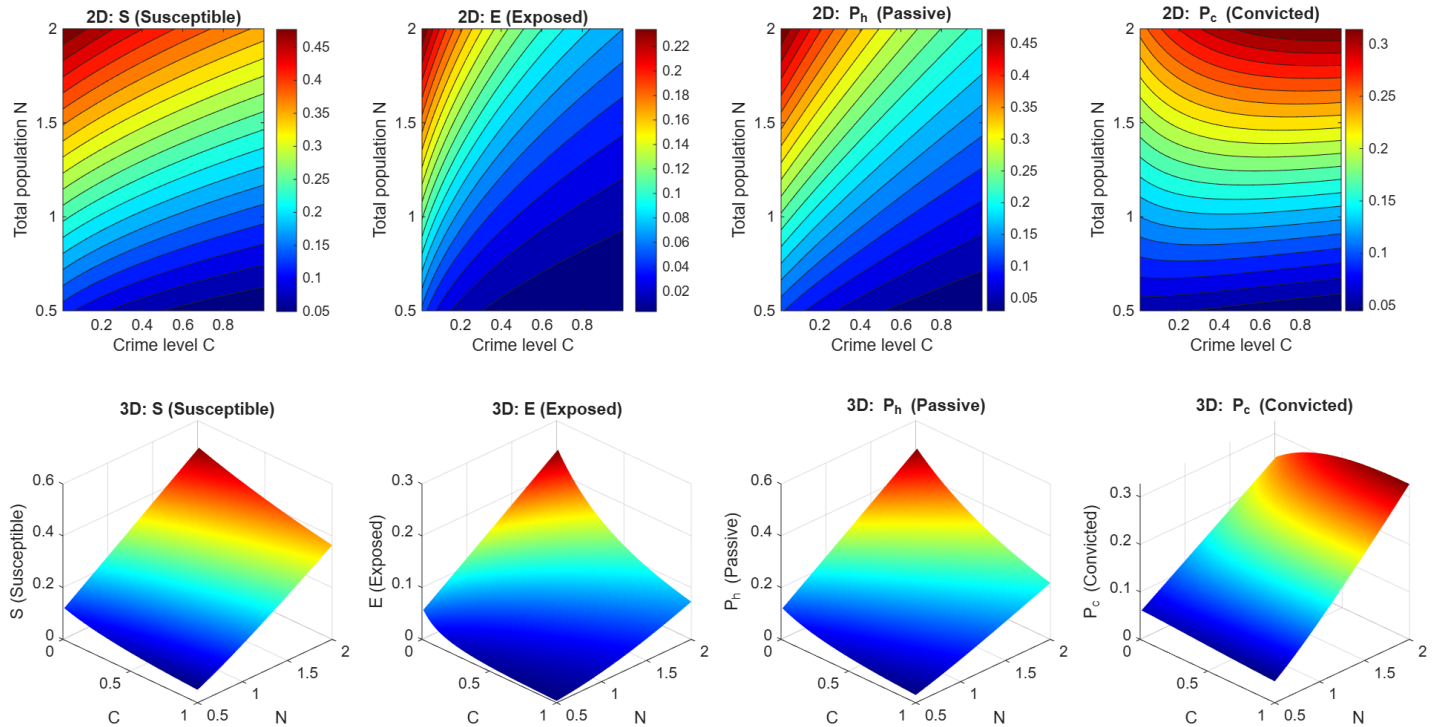


Figure 11. Combined two-dimensional contour plots (top row) and three-dimensional surface plots (bottom row) illustrating the Judicial-Absence Equilibrium (JAE) for four key compartments: susceptible individuals S , exposed individuals E , passive criminals P_h , and convicted criminals P_c . The equilibrium distributions are shown as functions of the crime level $C \in [0.01, 1]$ and the total population size $N \in [0.5, 2]$. These plots demonstrate how variations in crime intensity and population size influence compartmental equilibria in the absence of judicial enforcement, highlighting increased vulnerability and structural shifts in population composition.

- **Effect of δ_1 (Judicial Impact):** An increase in δ_1 produces a steady rise in \mathcal{R}_0 , suggesting that certain judicial processes, if not accompanied by strong deterrent measures, may inadvertently sustain crime cycles.
- **Effect of J_c^* (Equilibrium Corrupt Judges):** Higher values of J_c^* directly increase \mathcal{R}_0 , reflecting weakened judicial effectiveness. This indicates that corruption or inefficiency within the judiciary significantly contributes to the persistence of crime.

Overall, the sensitivity analysis reveals that the parameters μ , β_1 , and δ_1 exert the strongest influence on \mathcal{R}_0 . In particular, when $\mathcal{R}_0 > 1$, criminal activity is predicted to persist or grow within the population. Therefore, public policies aimed at increasing natural crime removal rates, reducing crime contact opportunities, and strengthening judicial integrity are crucial for maintaining $\mathcal{R}_0 < 1$ and ensuring long-term crime control.

6.5 Population Dynamics of the Crime Model under Judicial-Absence Equilibrium (JAE)

In this section, we investigate the population dynamics of the crime model under the *Judicial-Absence Equilibrium* (JAE), a scenario in which both judicial compartments, namely the honest judges J_h and corrupt judges J_c , are absent. This situation represents a breakdown of judicial processing or a failure of the legal system in which no active judicial intervention exists.

Under this assumption, the system simplifies considerably and admits explicit analytical expressions for the remaining population classes: Susceptible individuals (S), Exposed individuals (E), Passive criminals (P_h), and Convicted criminals (P_c), expressed as functions of the total population size N and the crime level C .

The model is evaluated using the following parameter

values:

$$\begin{aligned}\mu &= 0.1, & \beta_1 &= 0.3, & a_1 &= 0.1, & a_2 &= 0.15, \\ \eta_1 &= 0.05, & \kappa_1 &= 0.1, & \kappa_2 &= 0.1, & \beta_4 &= 0.2.\end{aligned}$$

Under the JAE assumption, the equilibrium expressions for each population class are given by

$$S(C, N) = \frac{\mu N^2}{\beta_1 C + \gamma N}, \quad (73)$$

$$E(C, N) = \frac{\eta_1 \mu N^2}{(\beta_1 C + \gamma N) \left(\mu + \frac{\beta_1 C}{N} \right)}, \quad (74)$$

$$\begin{aligned}P_h(C, N) &= \frac{a_2 \mu N^2 (\kappa_2 + \mu)}{(\beta_1 C + \gamma N)} \\ &\times \frac{1}{[(\kappa_2 + \mu)(\beta_4 C + \kappa_1 + \mu) - \kappa_2(\beta_4 C + \kappa_1)]}, \quad (75)\end{aligned}$$

$$P_c(C, N) = \frac{\beta_4 C + \kappa_1}{\kappa_2 + \mu} P_h(C, N). \quad (76)$$

where

$$\gamma = a_1 + a_2 + \eta_1 + \mu$$

represents the total outflow rate from the susceptible class.

Figure 11 presents combined two-dimensional contour plots and three-dimensional surface representations of the equilibrium populations as functions of the crime level C and the total population size N . The susceptible population S decreases steadily with increasing C , particularly for smaller values of N , indicating intensified transitions from susceptibility to exposed or criminal states as crime pressure grows. The exposed population E displays a non-monotonic pattern, reaching a maximum at intermediate crime levels and declining for larger C due to saturation effects and reduced inflow from the susceptible

class. The passive criminal population P_h remains comparatively small but increases gradually with both N and C , demonstrating the combined influence of population growth and crime propagation. Since the convicted criminal population P_c is directly proportional to P_h , it follows a similar qualitative trend while attaining higher magnitudes in densely populated environments. Overall, the JAE analysis highlights the critical role of judicial presence in regulating crime dynamics; in the absence of judicial control, criminal populations become highly sensitive to initial population size and crime contact rates, underscoring the necessity of effective enforcement and judicial mechanisms to prevent long-term crime escalation and systemic instability.

6.6 Behavior of the system's compartments over time

In this section, we investigate the temporal evolution of the extended crime dynamics model under different parameter scenarios using numerical simulations. The objective is to understand how variations in key socio-criminal and institutional parameters influence the evolution of the system over time. The behavior of the eight state variables—susceptible individuals (S), exposed individuals (E), criminals (C), convicted criminals (C_v), honest policymakers (P_h), corrupt policymakers (P_c), honest judiciary (J_h), and corrupt judiciary (J_c)—is analyzed through time-series plots. Each simulation highlights the dynamic interplay between crime propagation, enforcement mechanisms, and institutional integrity.

6.6.1 Impact of recruitment and exposure rates (μ, η_1)

Figure 12 illustrates the effect of increasing the natural recruitment rate μ and exposure rate η_1 on the system dynamics. Higher values of μ and η_1 initially increase the susceptible and exposed populations, which subsequently leads to a rise in criminal recruitment. Over time, the system approaches a dynamic balance where criminal activity and recovery processes coexist due to judicial and policy interventions. This behavior indicates that recruitment-driven crime growth can be

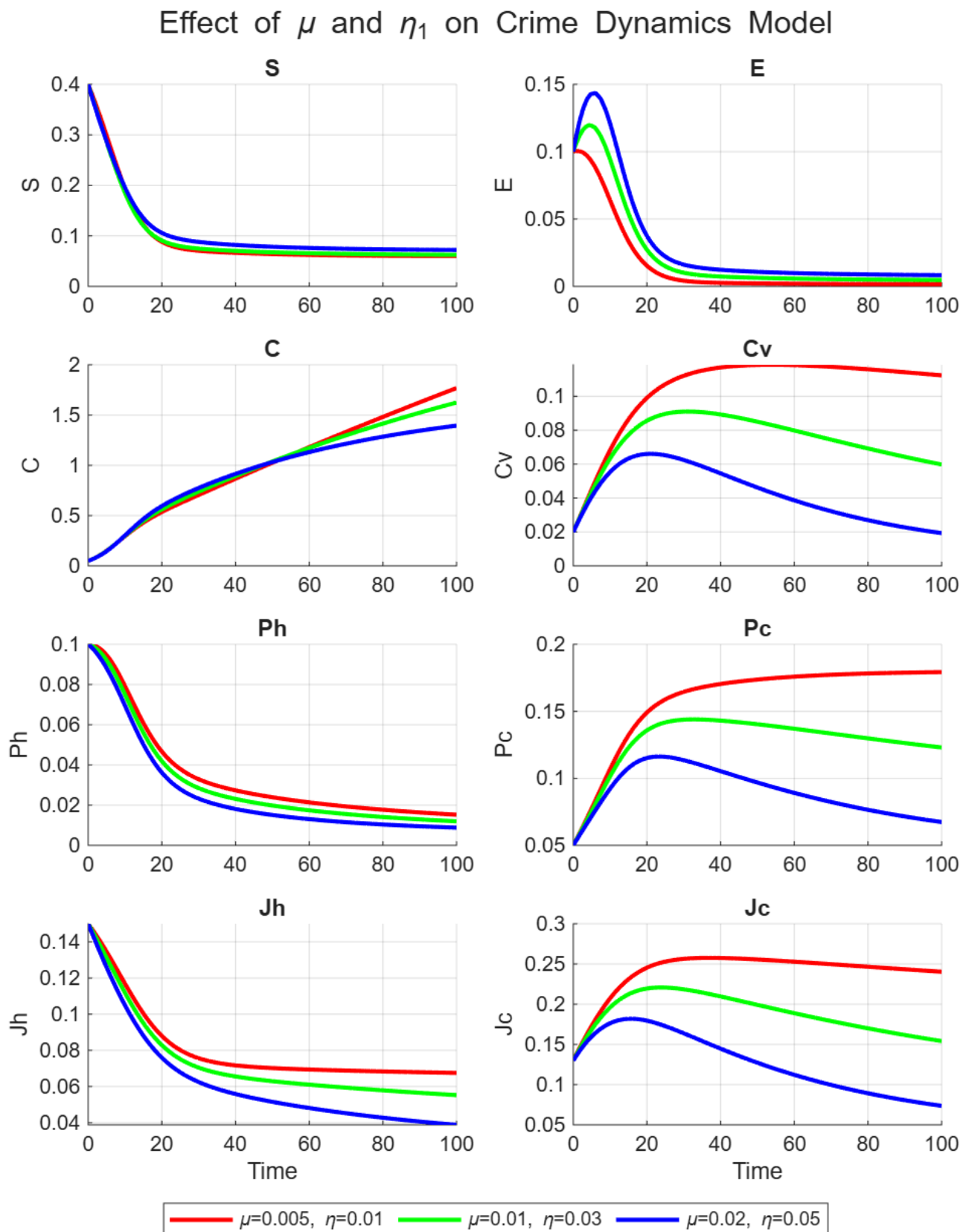


Figure 12. Time evolution of all state variables for different combinations of the natural death rate μ and susceptibility rate η_1 . The red, green, and blue curves correspond to the parameter sets $(\mu, \eta_1) = (0.005, 0.01)$, $(0.01, 0.03)$, and $(0.02, 0.05)$, respectively. The plots illustrate the transient and long-term dynamics of susceptible (S), exposed (E), active criminals (C), convicted criminals (C_v), passive-honest citizens (P_h), committed-honest citizens (P_c), honest judges (J_h), and corrupt judges (J_c). An increase in μ and η_1 accelerates population decay and suppresses institutional compartments, while lower values promote persistence and higher equilibrium levels.

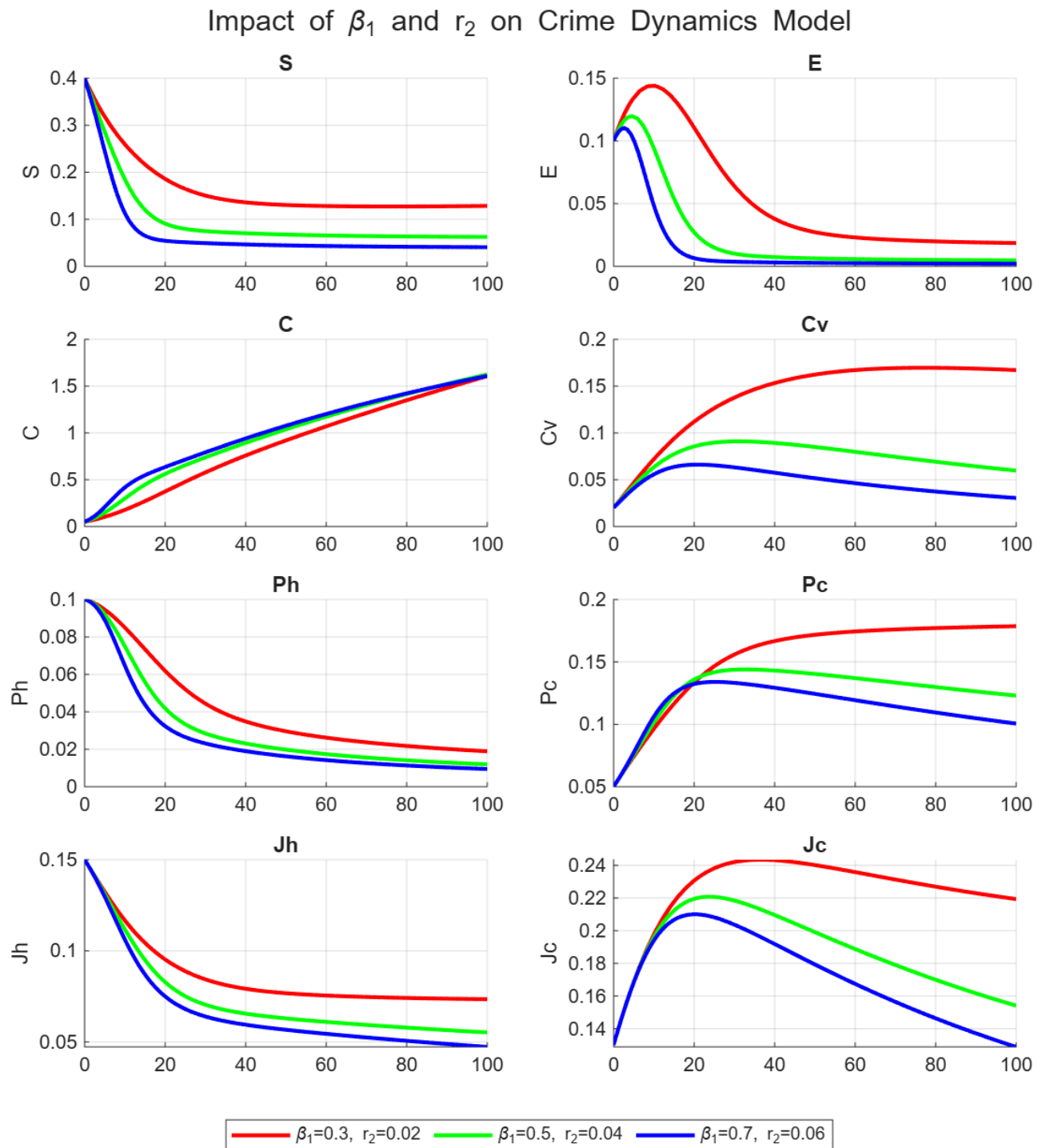


Figure 13. Time evolution of all state variables ($S, E, C, C_v, P_h, P_c, J_h, J_c$) for different values of the crime exposure rate β_1 and rehabilitation rate r_2 . Parameter sets considered are $(\beta_1, r_2) = (0.3, 0.02)$ (red), $(0.5, 0.04)$ (green), and $(0.7, 0.06)$ (blue), while all other parameters are held fixed. The results illustrate how stronger crime transmission and rehabilitation intensity jointly influence the transient and long-term dynamics of criminal, institutional, and judicial compartments.

mitigated through effective institutional responses.

6.6.2 Impact of crime transmission and conviction influence rates (β_1, r_2)

Figure 13 demonstrates the system dynamics under variations in the crime transmission rate β_1 and

the conviction influence rate r_2 . An increase in β_1 significantly amplifies the criminal population C by intensifying interactions between susceptible individuals and criminals.

While a higher r_2 accelerates the transition of criminals

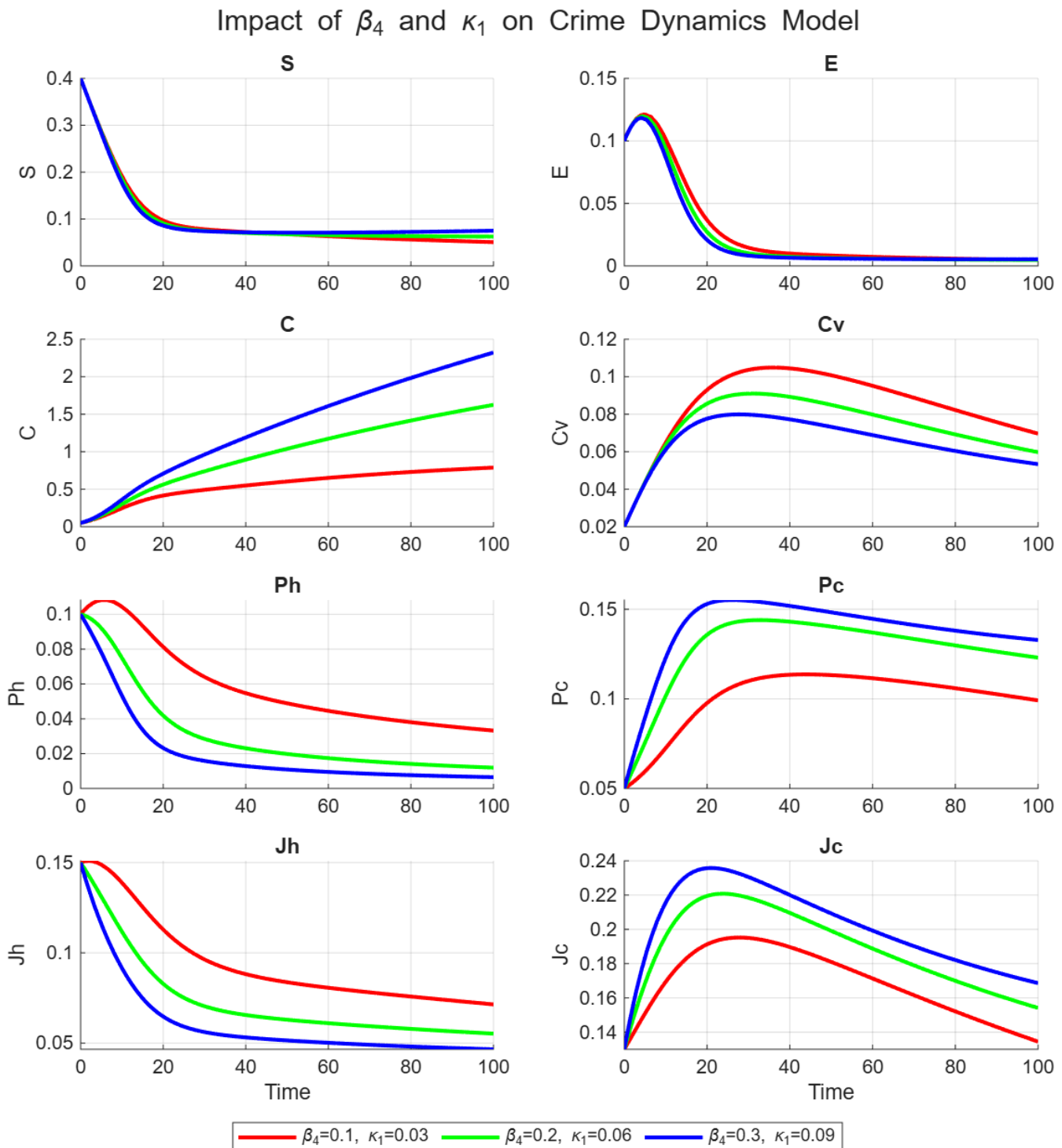


Figure 14. Time evolution of all compartments under varying policymaker corruption and institutional transition rates. The figure illustrates the impact of changes in the criminal influence on institutions β_4 and the transition rate between habitual and correctable states κ_1 on the dynamics of susceptible (S), exposed (E), criminals (C), convicted criminals (C_v), passive individuals (P_h), correctable individuals (P_c), honest judiciary (J_h), and corrupt judiciary (J_c). Parameter sets used are $(\beta_4, \kappa_1) = (0.1, 0.03)$ (red), $(0.2, 0.06)$ (green), and $(0.3, 0.09)$ (blue), while all other parameters are fixed.

to the convicted class C_v , it also introduces a feedback effect through institutional corruption, which may indirectly sustain criminal activity. Hence, the net impact of r_2 is nonlinear and context-dependent.

6.6.3 Impact of corruption rates among policymakers (β_4, κ_1)

Figure 14 presents the effect of varying the corruption-related parameters β_4 and κ_1 associated

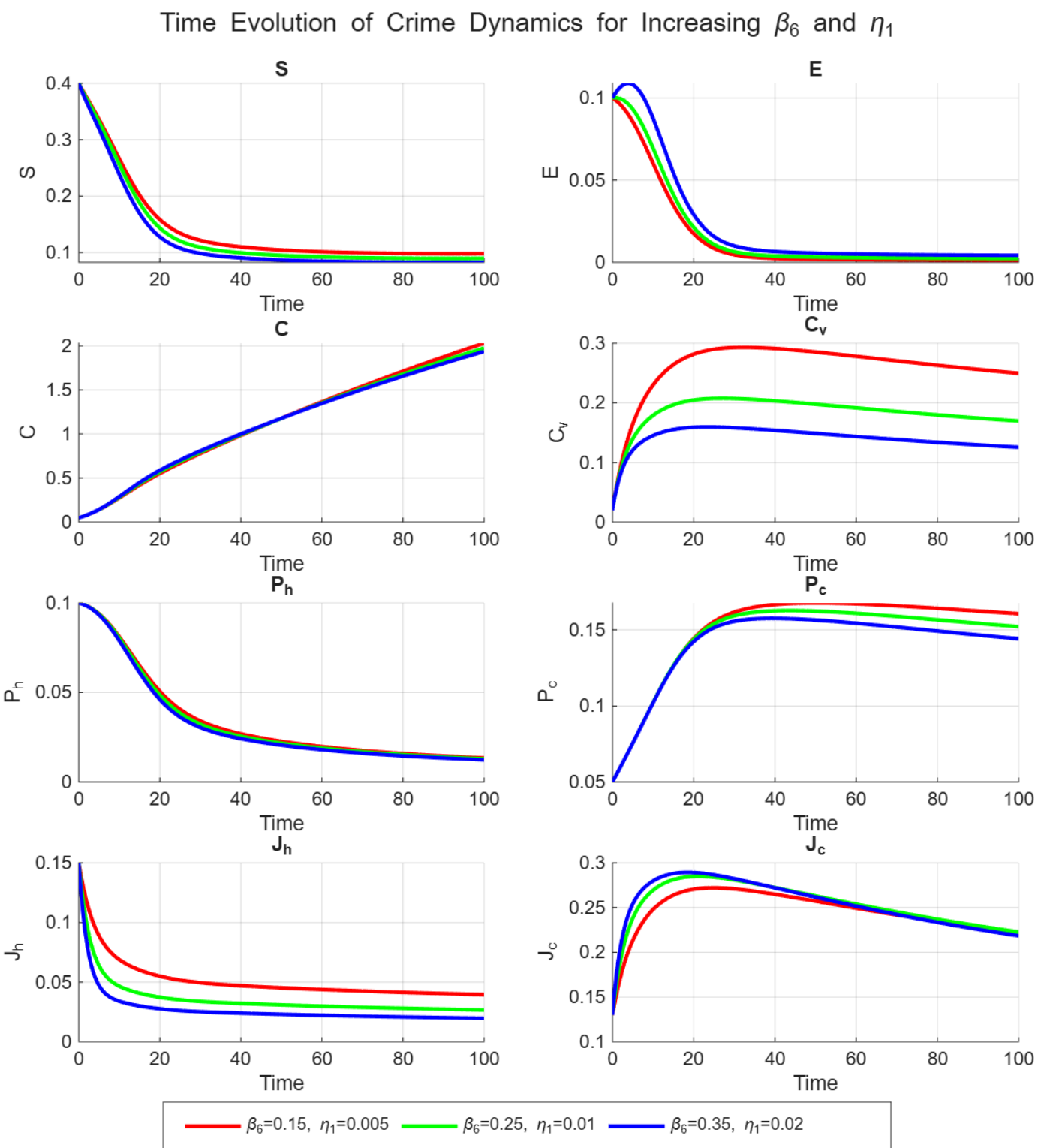


Figure 15. Time evolution of all population compartments for increasing values of the crime-judicial interaction rate β_6 and susceptibility parameter η_1 . The trajectories correspond to the parameter sets $(\beta_6, \eta_1) = (0.15, 0.005)$ (red), $(0.25, 0.01)$ (green), and $(0.35, 0.02)$ (blue). An increase in β_6 and η_1 accelerates the depletion of susceptible and honest populations (S, E, P_h, J_h), while amplifying criminal and correctional compartments (C, C_v, P_c, J_c), indicating enhanced crime propagation under higher exposure and institutional corruption effects.

with policymakers. An increase in these parameters leads to faster transitions from honest policymakers P_h to corrupt policymakers P_c . This shift weakens

law enforcement effectiveness, resulting in enhanced criminal activity and reduced deterrence. The results emphasize the critical role of political integrity in

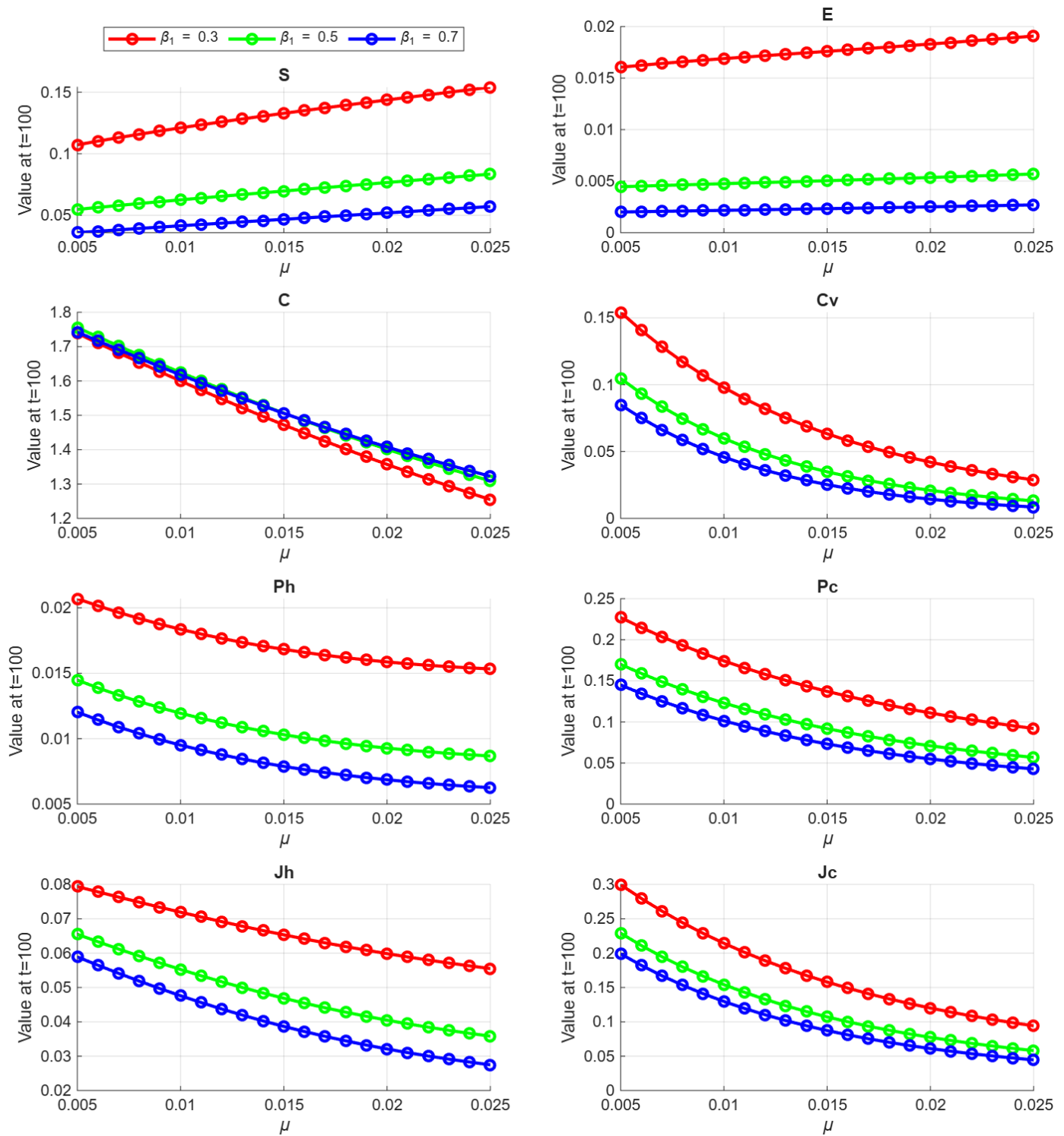


Figure 16. Variation of the equilibrium values of all population compartments at a fixed final time $t = 100$ with respect to the natural death rate μ for different values of the crime transmission rate $\beta_1 = 0.3$ (red), $\beta_1 = 0.5$ (green), and $\beta_1 = 0.7$ (blue). Each subplot corresponds to a distinct compartment: susceptible individuals S , exposed individuals E , criminals C , convicted criminals C_v , honest police P_h , corrupt police P_c , honest judiciary J_h , and corrupt judiciary J_c . The results illustrate the combined influence of demographic turnover and crime exposure intensity on the long-term population distribution.

controlling crime dynamics.

6.6.4 Impact of judicial corruption and cooperation with crime (β_6, δ_1)

Figure 15 highlights the consequences of judicial corruption parameters β_6 and δ_1 on the evolution of the system. Higher values of β_6 accelerate the transition from honest judges J_h to corrupt judges J_c , thereby strengthening criminal support from within the judiciary. The parameter δ_1 directly contributes to the growth of the criminal population, particularly in the presence of a large corrupt judiciary class. This reveals a detrimental feedback loop between crime and judicial failure. Overall, these numerical simulations demonstrate that increases in corruption-related parameters consistently elevate criminal and corrupt compartments, whereas enhancements in recovery, conviction, and institutional enforcement parameters tend to stabilize or reduce criminality. The results underscore the critical importance of systemic integrity and coordinated institutional control in mitigating long-term crime dynamics.

6.7 Impact of μ on system dynamics for varying β_1

Figure 16 illustrates the combined influence of the natural removal rate μ and the crime transmission rate β_1 on the long-term population distributions at time $t = 100$. As μ increases, the susceptible and exposed populations (S, E) exhibit a gradual increase, particularly for lower values of β_1 , reflecting reduced criminal transmission under stronger removal mechanisms. In contrast, both the criminal (C) and convicted (C_v) populations decline sharply with increasing μ , with the effect being more pronounced for higher β_1 , where crime transmission is initially stronger. All law-enforcement and judicial compartments (P_h, P_c, J_h, J_c) also decrease as μ grows, indicating reduced institutional pressure when criminal activity weakens. However, larger values of β_1 consistently sustain higher criminal and conviction levels even for moderate μ , highlighting that suppressing crime transmission is as crucial as enhancing removal or rehabilitation. Overall, the results in Figure 16 demonstrate a nonlinear interplay between μ and β_1 , emphasizing that effective

long-term crime control requires simultaneous reduction of criminal transmission and strengthening of removal and rehabilitation processes.

6.8 Impact of varying the arrest rate parameters a_1 and a_2

Figure 17 illustrates the impact of varying the arrest rate parameter a_1 on the system dynamics at a fixed time $t = 100$, for three different values of the rehabilitation rate $a_2 \in \{0.01, 0.03, 0.05\}$. Each subplot corresponds to one of the eight model compartments: susceptible (S), exposed (E), criminals (C), convicted criminals (C_v), passive honest individuals (P_h), committed honest individuals (P_c), honest judges (J_h), and corrupt judges (J_c). The numerical results show that both the susceptible and exposed populations increase with higher arrest rates a_1 , indicating that stronger enforcement slows the immediate transition into active criminality, while the influence of a_2 on these compartments remains comparatively mild. The criminal population (C) grows with increasing a_1 but declines as a_2 increases, revealing a trade-off between enforcement intensity and effective rehabilitation. The convicted class (C_v) is highly sensitive to both parameters and reaches its largest values when arrest and rehabilitation rates are simultaneously high, emphasizing their joint role in transferring individuals from crime to conviction. Both honest populations (P_h, P_c) increase with a_1 , with P_c responding more strongly to changes in a_2 , highlighting the importance of rehabilitation in sustaining committed honest behavior. Finally, the judicial compartments (J_h, J_c) expand with increasing a_1 , especially for larger a_2 , suggesting that intensified enforcement and reform place greater demands on judicial institutions and may accelerate internal transitions, including the emergence of corruption. Overall, Figure 17 demonstrates that while higher arrest rates intensify criminal justice involvement, coordinated rehabilitation efforts are essential to counterbalance this effect and promote long-term crime reduction and social stability.

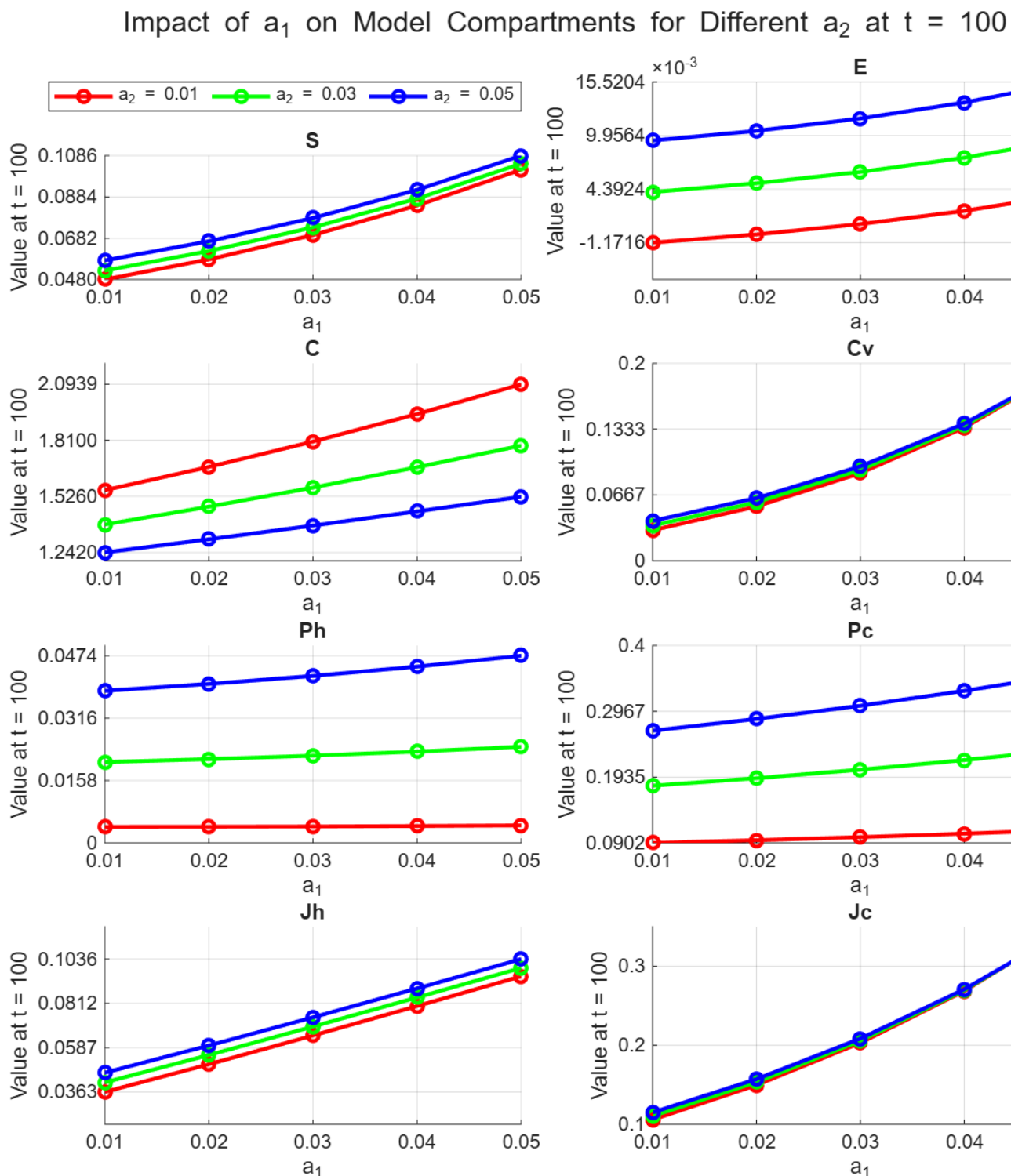


Figure 17. Time-asymptotic values of all model compartments at fixed time $t = 100$ as functions of the arrest rate a_1 for three different rehabilitation rates: $a_2 = 0.01$ (red), $a_2 = 0.03$ (green), and $a_2 = 0.05$ (blue). Each subplot corresponds to one compartment of the model: susceptible individuals S , exposed individuals E , criminals C , convicted criminals C_v , honest police P_h , corrupt police P_c , honest judiciary J_h , and corrupt judiciary J_c .

6.9 Results and Discussion: Joint Impact of β_2 and δ_1

Figure 18 illustrates the combined influence of law enforcement effectiveness β_2 and the interaction

strength between honest and corrupt judges δ_1 on the long-term dynamics of the crime-justice system through contour plots of all eight population compartments evaluated at $t = 100$ for $\beta_2 \in$

Contour plots of population compartments at $t = 100$ w.r.t. β_2 and δ_1

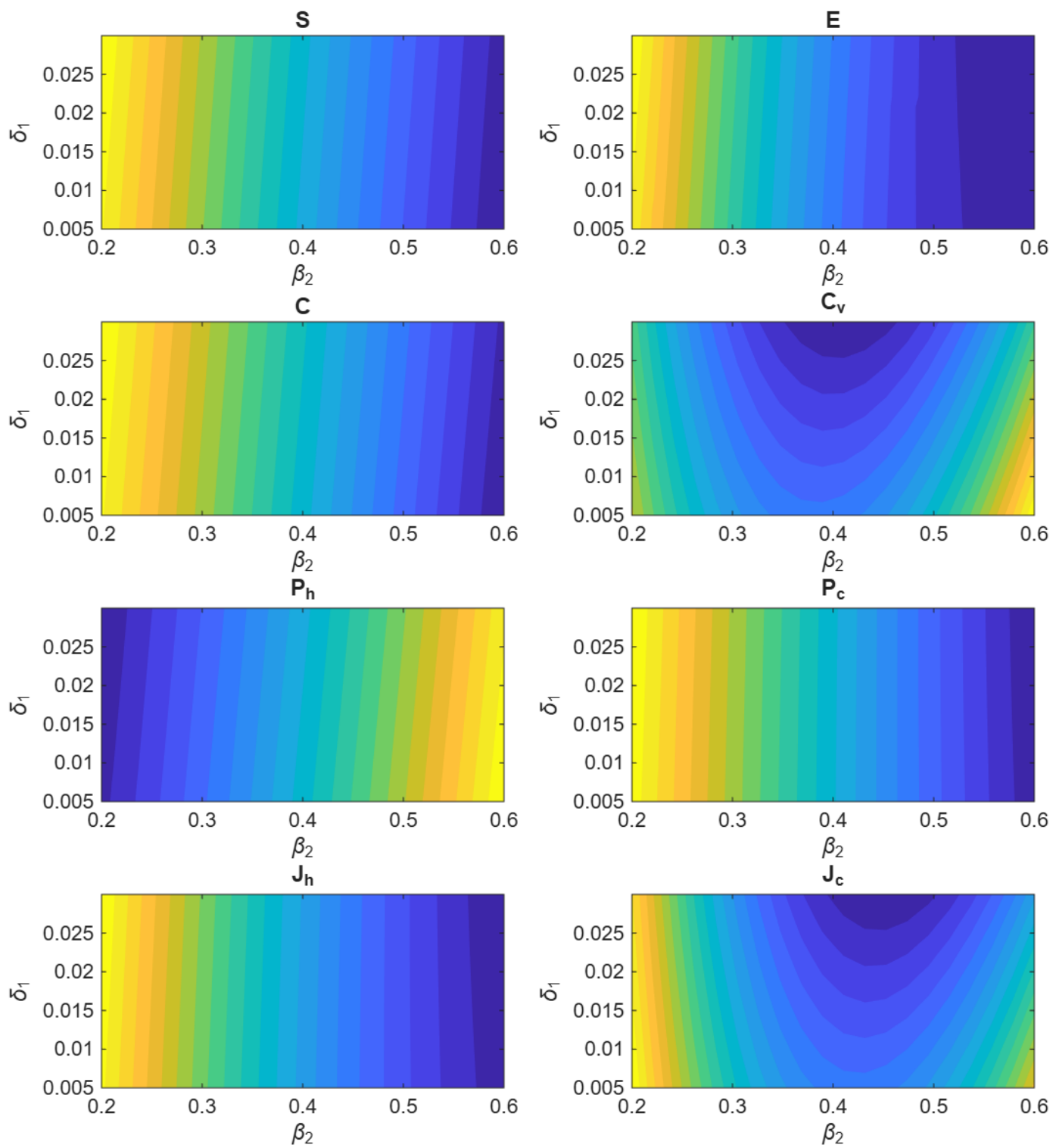


Figure 18. Contour plots of population compartments at $t = 100$ with respect to variations in the crime transmission rate β_2 and judicial deterrence parameter δ_1 . Each subplot represents the steady-state value of a specific compartment: Susceptible individuals (S), Exposed individuals (E), Criminals (C), Convicted criminals (C_v), Passive honest police (P_h), Committed honest police (P_c), Honest judges (J_h), and Corrupt judges (J_c). The color gradients illustrate the sensitivity of each compartment to joint changes in crime transmission and judicial intervention intensity.

$[0.2, 0.6]$ and $\delta_1 \in [0.005, 0.03]$. The susceptible and exposed populations show only mild sensitivity to these parameters, with larger values of δ_1 slightly reducing S and increasing E , indicating that judicial

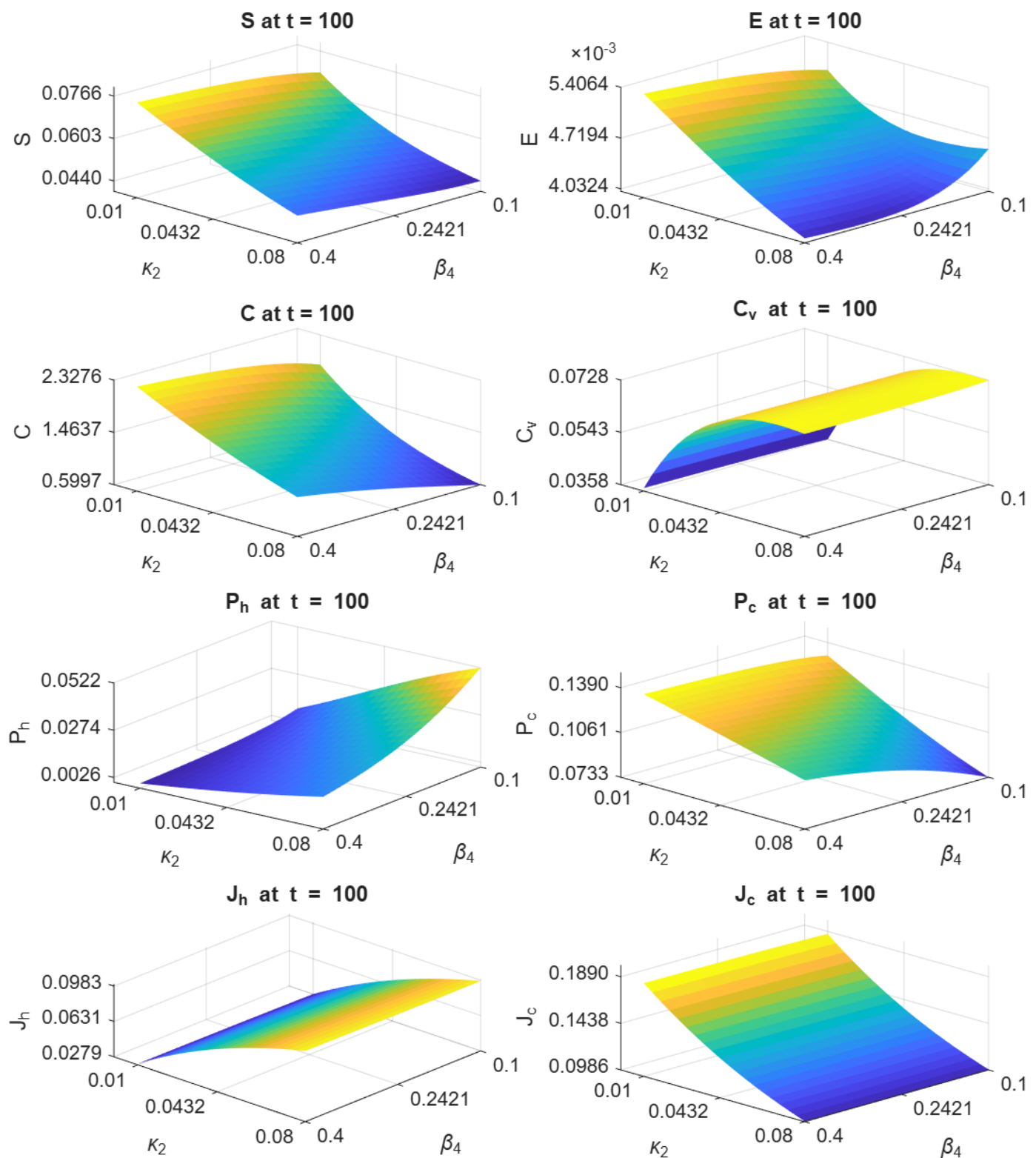


Figure 19. Three-dimensional surface plots illustrating the combined impact of the corruption influence rate β_4 (x-axis) and the judicial correction rate κ_2 (y-axis) on the steady-state population compartments at time $t = 100$. Each subplot corresponds to one compartment of the model: susceptible individuals (S), exposed individuals (E), criminals (C), convicted criminals (C_v), passive honest police (P_h), committed honest police (P_c), honest judges (J_h), and corrupt judges (J_c). The surfaces reveal the nonlinear sensitivity of institutional and population dynamics to variations in corruption pressure and judicial efficiency.

corruption indirectly raises exposure by weakening C responds strongly: increasing β_2 significantly deterrence. In contrast, the criminal population suppresses crime due to more effective enforcement,

whereas higher δ_1 promotes criminal persistence by undermining judicial credibility. A similar interaction is observed for convicted criminals C_v , whose levels rise with δ_1 but display a non-monotonic dependence on β_2 , suggesting saturation effects under corrupt institutional conditions. Among the honest subpopulations, passive honest individuals P_h decline as δ_1 increases, reflecting erosion of public trust, while the committed honest group P_c exhibits a more complex nonlinear response driven by competing enforcement and corruption effects. The judicial compartments are the most sensitive: honest judges J_h decrease sharply with increasing δ_1 , whereas corrupt judges J_c expand rapidly, confirming the dominant role of judicial corruption in reshaping institutional integrity. Overall, Figure 18 demonstrates that although strengthening law enforcement (β_2) is effective in reducing crime, its benefits are substantially weakened when judicial corruption (δ_1) is high, highlighting the need for integrated policies that simultaneously enhance enforcement capacity and protect judicial integrity to achieve sustainable crime reduction.

6.10 3D Surface Analysis of the Impact of β_4 and κ_2

Figure 19 illustrates the combined influence of the crime-honest interaction rate β_4 and the judicial transition rate κ_2 on the long-term behavior of the extended crime-justice system, using three-dimensional surface plots of all eight population compartments evaluated at $t = 100$ for $\beta_4 \in [0.1, 0.4]$ and $\kappa_2 \in [0.01, 0.08]$. The susceptible and exposed populations vary only mildly across the parameter space, with larger κ_2 generally reducing both due to faster institutional transitions, while β_4 has a weaker effect. In contrast, the criminal population C decreases noticeably as β_4 increases, reflecting stronger interactions with honest individuals, although higher κ_2 can counteract this reduction in certain regions by destabilizing committed honesty and enabling indirect criminal resurgence; the convicted class C_v responds accordingly. The honest subpopulations show complementary behavior: the committed honest

group P_c grows with κ_2 , indicating enhanced recovery and institutional reinforcement, whereas the passive honest group P_h generally declines as individuals transition toward stronger civic engagement or other states. Judicial compartments are the most sensitive, with both honest judges J_h and corrupt judges J_c exhibiting pronounced nonlinear responses to κ_2 , revealing regions where either integrity or corruption dominates. Overall, Figure 19 highlights the strong interplay between social interaction dynamics (β_4) and institutional transition mechanisms (κ_2), underscoring that effective crime-control strategies must jointly strengthen civic engagement and judicial reform rather than targeting either mechanism in isolation.

6.11 Impact of μ and ρ_2 on Equilibrium States

Figure 20 depicts the sensitivity of the equilibrium states to variations in the natural death rate μ , with the total population fixed at $N = 500$ and the active criminal population at $C = 100$, for three levels of social reinforcement $\rho_2 = \{0.05, 0.10, 0.15\}$. As μ increases over $[0.005, 0.1]$, the susceptible population S^* increases steadily across all ρ_2 , reflecting reduced progression into other compartments and enhanced social stability under stronger feedback. In contrast, the honest judge population J_h^* decreases nonlinearly with μ , as higher mortality weakens judicial recruitment and retention; however, this decline is partially alleviated for larger ρ_2 , underscoring the stabilizing role of social reinforcement. The corrupt judge population J_c^* also declines with increasing μ , though more gradually than J_h^* , suggesting that corruption may persist longer under high mortality and weak feedback. Similarly, the convicted criminal population C_v^* drops sharply as μ rises, particularly for small ρ_2 , indicating reduced conviction accumulation when social feedback is weak. Overall, Figure 20 highlights that while increased mortality suppresses criminal and judicial compartments, strong social reinforcement is crucial for sustaining institutional stability and preventing long-term persistence of corruption.

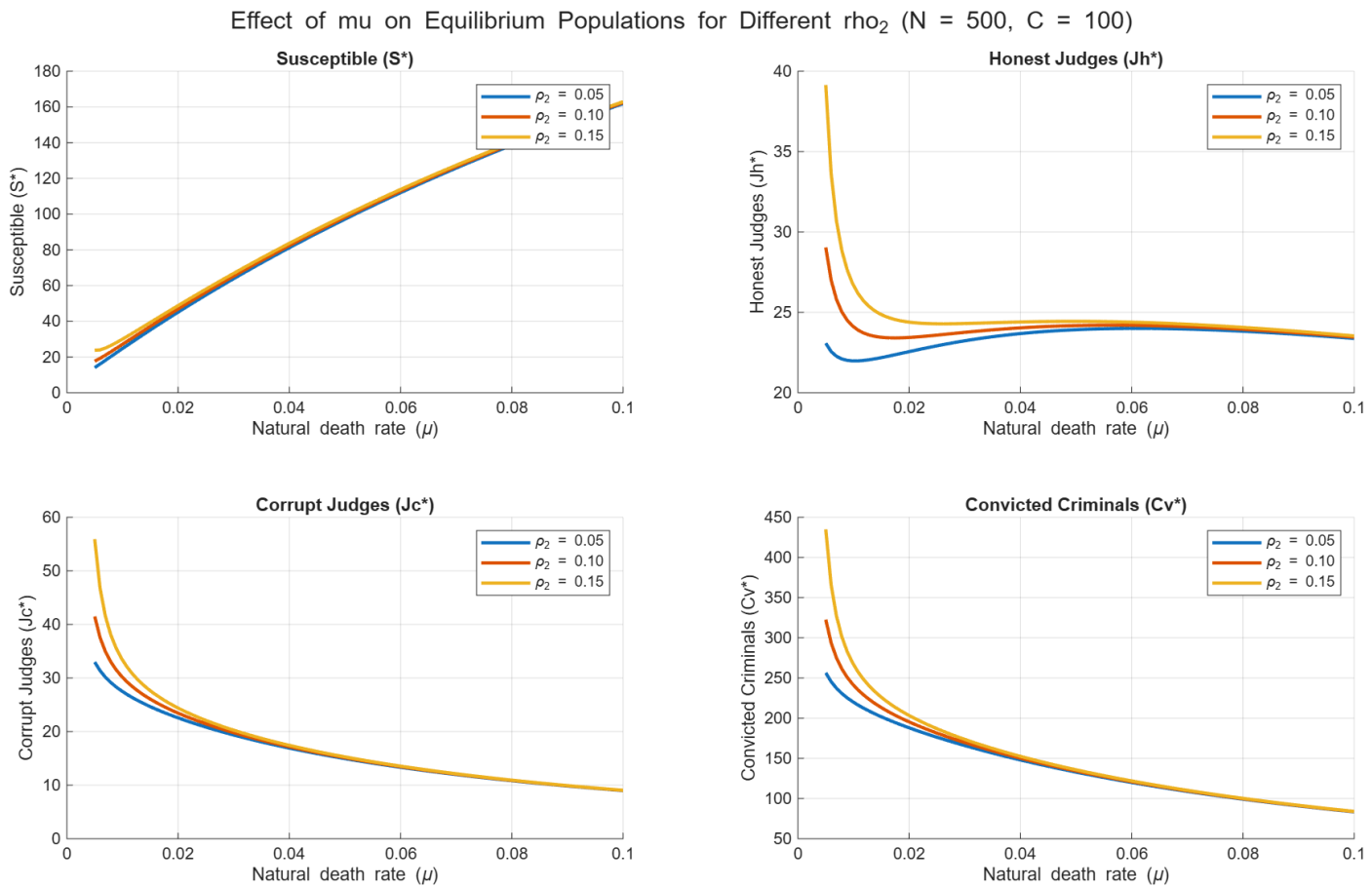


Figure 20. Effect of varying the natural death rate μ on equilibrium population levels for different values of the institutional reinforcement parameter ρ_2 . The plots illustrate the equilibrium susceptible population S^* , honest judges J_h^* , corrupt judges J_c^* , and convicted criminals C_v^* as functions of μ . Results are shown for $\rho_2 \in \{0.05, 0.10, 0.15\}$, with total population $N = 500$ and initial criminal population $C = 100$ fixed.

6.12 Impact of Exposure Rate η_1 on Equilibrium Populations

Figure 21 illustrates the sensitivity of the equilibrium populations to variations in the exposure rate η_1 , which represents social vulnerability to crime. The parameter η_1 is varied over $[0.005, 0.1]$ while fixing $N = 500$ and $C = 100$, and considering three levels of social reinforcement $\rho_2 = \{0.05, 0.10, 0.15\}$. As η_1 increases, the susceptible population S^* decreases monotonically, reflecting the direct impact of higher exposure in reducing the pool of unexposed individuals; this decline is more pronounced for smaller values of ρ_2 . The honest judge population J_h^* exhibits a nonlinear decrease with increasing η_1 due to weakened recruitment from the susceptible class, although this effect is partially mitigated under stronger social reinforcement. The corrupt judge population J_c^* also declines with η_1 but with weaker sensitivity, indicating

that exposure primarily disrupts honest institutional pathways rather than directly accelerating corruption. Similarly, the convicted criminal population C_v^* decreases as higher exposure overwhelms corrective mechanisms, particularly when social reinforcement is weak. Overall, Figure 21 highlights the destabilizing role of increased exposure on institutional stability and emphasizes the buffering effect of strong social reinforcement and post-conviction support in sustaining long-term societal equilibrium.

6.13 Impact of Recruitment Parameters a_1 and a_2 on System Equilibrium

In Figure 22, we examine the effect of recruitment in judicial and police institutions on the long-term equilibrium of the system by varying the recruitment rates of honest judges (a_1) and honest police officers (a_2) over the range $[0.01, 0.05]$. All other parameters

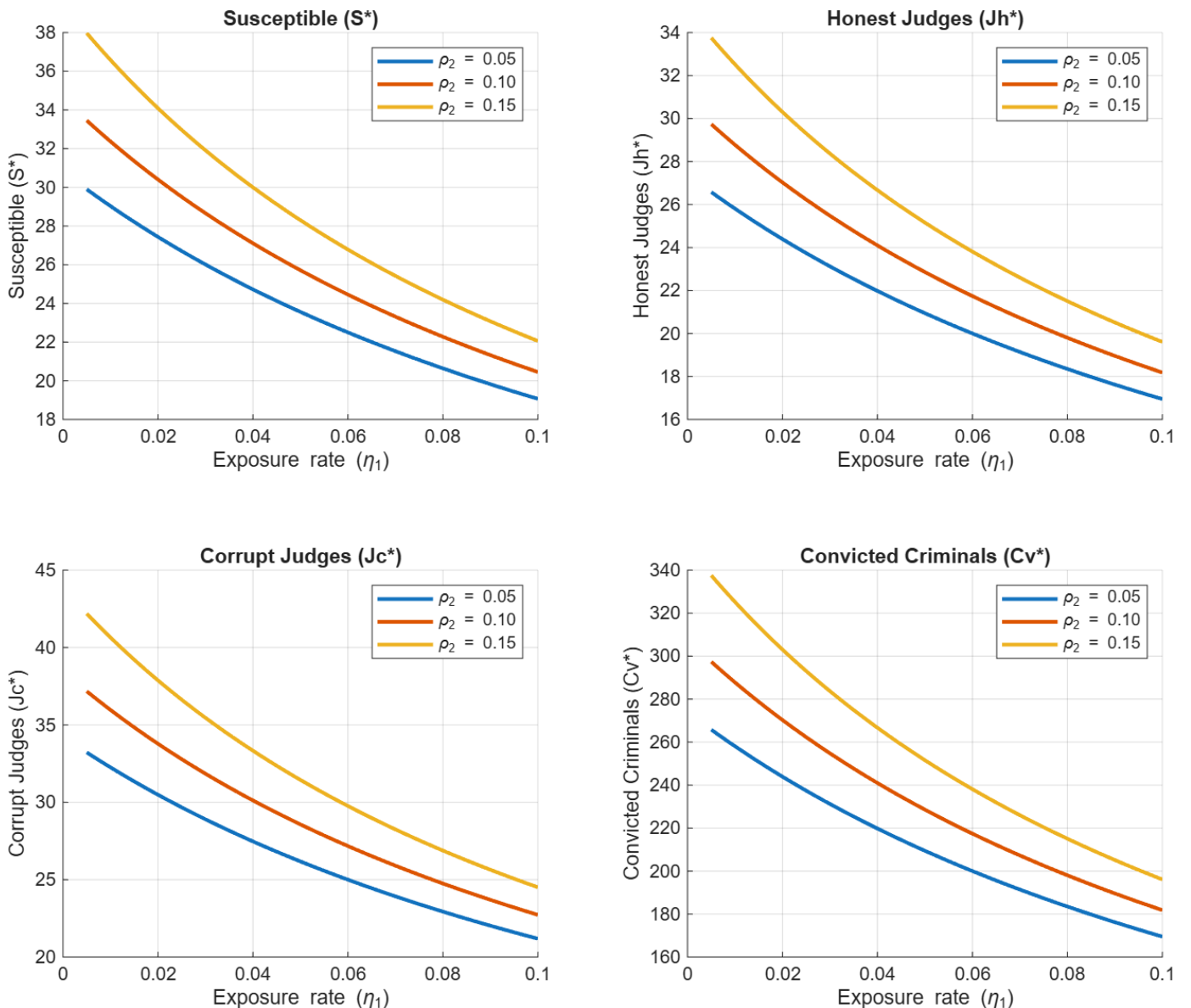


Figure 21. Effect of varying the exposure rate η_1 on equilibrium population levels for different values of social reinforcement ρ_2 . The panels show the equilibrium values of susceptible individuals (S^*), honest judges (J_h^*), corrupt judges (J_c^*), and convicted criminals (C_v^*) as functions of η_1 . Three values of ρ_2 are considered: $\rho_2 = 0.05$ (blue), $\rho_2 = 0.10$ (red), and $\rho_2 = 0.15$ (yellow). Fixed parameters are $N = 500$, $C = 100$, $\mu = 0.01$, $a_1 = 0.02$, $a_2 = 0.03$, $\beta_1 = 0.6$, $\beta_3 = 0.5$, $r_2 = 0.04$, $\kappa_1 = 0.05$, and $\kappa_2 = 0.03$.

are fixed with total population $N = 500$, active criminals $C = 100$, $\mu = 0.01$, $\eta_1 = 0.03$, $\beta_1 = 0.6$, $\beta_3 = 0.5$, $r_2 = 0.04$, $\rho_2 = 0.1$, and $\kappa_1 = 0.05$, $\kappa_2 = 0.03$. The results show that the equilibrium susceptible population S^* decreases as both a_1 and a_2 increase, indicating that stronger institutional recruitment reduces societal susceptibility. The equilibrium level of honest judges J_h^* rises sharply with a_1 and is only weakly affected by a_2 , consistent with direct judicial recruitment from the susceptible class. As a consequence of increased

judicial inflow, the corrupt judge population J_c^* also increases with a_1 , while remaining relatively insensitive to a_2 . The convicted criminal population C_v^* grows with increasing a_1 , reflecting enhanced judicial capacity, but its growth slows or slightly declines for larger a_2 , suggesting that police recruitment alone is insufficient to sustain long-term conviction levels without parallel judicial strengthening. Overall, the contour analysis highlights the synergistic role of coordinated recruitment in judicial and police sectors, where balanced investment in both yields the most

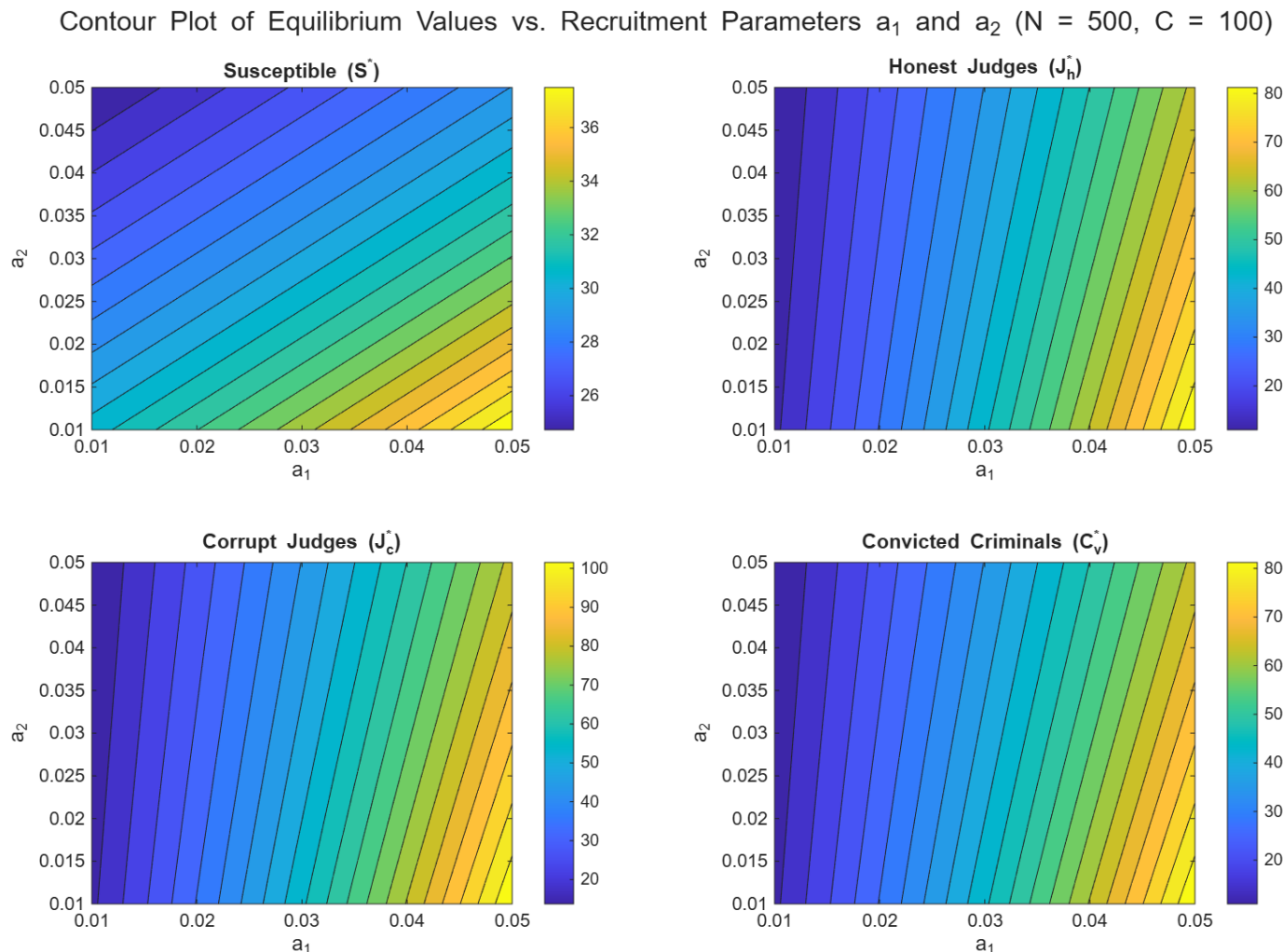


Figure 22. Contour plots illustrating the equilibrium values of key population compartments as functions of the recruitment parameters a_1 and a_2 . The panels correspond to the susceptible population (S^*), honest judges (J_h^*), corrupt judges (J_c^*), and convicted criminals (C_v^*). Warmer colors indicate higher equilibrium levels. Fixed parameter values are

$N = 500$, $C = 100$, $\mu = 0.01$, $\eta_1 = 0.03$, $\beta_1 = 0.6$, $\beta_3 = 0.5$, $r_2 = 0.04$, $\rho_2 = 0.1$, $\kappa_1 = 0.05$, and $\kappa_2 = 0.03$.

effective crime control outcomes.

Conclusion

This study presented an extended nonlinear compartmental model to investigate and predict the dynamics of crime in society. The proposed framework integrates multiple interacting subpopulations, including susceptible individuals, exposed individuals, active criminals, convicted criminals, passive and committed honest citizens, and judicial actors (honest and corrupt judges). By incorporating recruitment, exposure, correction, corruption, and judicial transitions, the model captures essential societal mechanisms governing real-world crime dynamics. Analytical results established the positivity

and boundedness of solutions under biologically meaningful parameter constraints. A crime-free equilibrium was derived, and its local stability was examined using Jacobian-based eigenvalue analysis. These findings revealed the critical roles of recruitment, attrition, and transition rates in shaping the system's stability landscape. A comprehensive set of numerical simulations—including time-series analysis, parametric line plots, contour maps, and three-dimensional surface visualizations—was conducted to explore the long-term impact of key parameters. The main findings can be summarized as follows:

- **Stabilization and Crime-Free Behavior:** Time-series simulations demonstrated that

the system converges to equilibrium within a finite time horizon (approximately $t \approx 100$), validating the relevance of steady-state analysis for long-term policy evaluation.

- **Sensitivity to Core Parameters:** The evolution of criminal and honest populations is highly sensitive to the natural death rate μ , exposure rate η_1 , and crime transmission rate β_1 . In particular, increases in β_1 consistently led to higher criminal prevalence, emphasizing the importance of limiting crime contact mechanisms.
- **Impact of Institutional Mechanisms:** Parameters associated with institutional strength—such as judicial recruitment (a_1, a_2), commitment transitions (κ_1, κ_2), and recidivism control (r_1, r_2)—play a decisive role in suppressing crime and reinforcing honest subpopulations.
- **Effects of Reinforcement and Corruption:** Social and judicial reinforcement parameters (ρ_1, ρ_2) improve system outcomes by reducing criminal activity, whereas high corruption feedback (δ_1) erodes judicial integrity. This highlights the delicate balance between governance strength and institutional decay.
- **Nonlinear and Threshold Behavior:** Contour and three-dimensional surface analyses revealed nonlinear relationships and threshold effects in population transitions, suggesting bifurcation-like behavior and underscoring the importance of parameter tuning in crime control strategies.

In summary, this work provides a robust theoretical and computational framework for understanding crime dynamics in complex social systems. The results demonstrate that targeted interventions—particularly those strengthening social reinforcement, judicial integrity, and coordinated institutional recruitment—can substantially alter long-term outcomes. These findings offer valuable insights for designing effective crime prevention policies and enhancing societal resilience against

criminal proliferation.

Data Availability Statement

Data will be made available on request.

Funding

This work was supported without any funding.

Conflicts of Interest

The authors declare no conflicts of interest.

AI Use Statement

The authors declare that no generative AI was used in the preparation of this manuscript.

Ethical Approval and Consent to Participate

Not applicable. This is a theoretical mathematical modeling study using only publicly available aggregated data; no human participants were involved.

References

- [1] United Nations. (2003). Manual for the Development of a System of Criminal Justice Statistics (Series F, No. 89). United Nations Statistics Division. Retrieved from <https://unstats.un.org/unsd/methods/crime/>
- [2] Law, J. (Ed.). (2015). *A dictionary of law*. OUP Oxford.
- [3] Schabbach, L. M. (2013). O crime organizado em perspectiva mundial. *Sociologias*, 15, 278–293. [CrossRef]
- [4] Balhara, Y. P. S., Sarkar, S., & Rajguru, A. J. (2024). Drug-related offences in India: Observations and insights from the secondary analysis of the data from the National Crimes Record Bureau. *Indian Journal of Psychological Medicine*, 46(6), 527-534. [CrossRef]
- [5] McMillon, D., Simon, C. P., & Morenoff, J. (2014). Modeling the underlying dynamics of the spread of crime. *PloS one*, 9(4), e88923. [CrossRef]
- [6] National Association for the Advancement of Colored People. (2011). *Misplaced priorities: Over incarcerate, under educate Excessive spending on incarceration undermines educational opportunity and public safety in*

communities. National Institute of Justice. Retrieved from <https://www.ncjrs.gov/App/Publications/abstract.aspx?ID=256929>

[7] Wilson, J. Q., & Herrnstein, R. J. (1985). *Crime and human nature*. Simon and Schuster.

[8] Bandura, A., & Walters, R. H. (1977). *Social learning theory* (Vol. 1, pp. 141-154). Englewood Cliffs, NJ: Prentice hall.

[9] Becker, G. S. (1968). Crime and punishment: An economic approach. *Journal of political economy*, 76(2), 169-217. [\[CrossRef\]](#)

[10] Burdett, K., Lagos, R., & Wright, R. (2004). An on-the-job search model of crime, inequality, and unemployment. *International Economic Review*, 45(3), 681-706. [\[CrossRef\]](#)

[11] McMillon, D., Morenoff, J., Simon, C., & Lane, E. (2025). A dynamical systems analysis of criminal behavior using national longitudinal survey of youth data. *Plos one*, 20(8), e0324014. [\[CrossRef\]](#)

[12] Short, M. B., Bertozzi, A. L., & Brantingham, P. J. (2010). Nonlinear patterns in urban crime: Hotspots, bifurcations, and suppression. *SIAM Journal on Applied Dynamical Systems*, 9(2), 462-483. [\[CrossRef\]](#)

[13] Rodriguez, N., & Bertozzi, A. (2010). Local existence and uniqueness of solutions to a PDE model for criminal behavior. *Mathematical Models and Methods in Applied Sciences*, 20(supp01), 1425-1457. [\[CrossRef\]](#)

[14] Manasevich, R., Phan, Q. H., & Souplet, P. (2013). Global existence of solutions for a chemotaxis-type system arising in crime modelling. *European Journal of Applied Mathematics*, 24(2), 273-296. [\[CrossRef\]](#)

[15] Cantrell, R. S., Cosner, C., & Manásevich, R. (2012). Global bifurcation of solutions for crime modeling equations. *SIAM Journal on Mathematical Analysis*, 44(3), 1340-1358. [\[CrossRef\]](#)

[16] Mohler, G. O., & Short, M. B. (2012). Geographic profiling from kinetic models of criminal behavior. *SIAM Journal on Applied Mathematics*, 72(1), 163-180. [\[CrossRef\]](#)

[17] Misra, A. (2014). Modeling the effect of police deterrence on the prevalence of crime in the society. *Applied Mathematics and Computation*, 237, 531-545. [\[CrossRef\]](#)

[18] Diekmann, O., Heesterbeek, J. A. P., & Roberts, M. G. (2010). The construction of next-generation matrices for compartmental epidemic models. *Journal of the royal society interface*, 7(47), 873-885. [\[CrossRef\]](#)

[19] Bansal, S., Grenfell, B. T., & Meyers, L. A. (2007). When individual behaviour matters: homogeneous and network models in epidemiology. *Journal of the Royal Society Interface*, 4(16), 879-891. [\[CrossRef\]](#)

[20] Van den Driessche, P., & Watmough, J. (2002). Reproduction numbers and sub-threshold endemic equilibria for compartmental models of disease transmission. *Mathematical Biosciences*, 180(1-2), 29-48. [\[CrossRef\]](#)

[21] Glaeser, E. L., Sacerdote, B., & Scheinkman, J. A. (1996). Crime and social interactions. *The Quarterly Journal of Economics*, 111(2), 507-548. [\[CrossRef\]](#)

[22] Pippal, S., Kapoor, S., & Ranga, A. (2025). Bifurcation and stability analysis with numerical simulations of a social model for marriage and divorce under fear effect. *Nonlinear Science and Control Engineering*, 1(1), 025290005. [\[CrossRef\]](#)

[23] National Crime Records Bureau, Ministry of Home Affairs. (2023). *Crime in India 2022: Statistics (Volume-1)*. Government of India. Retrieved from https://images.assettype.com/barandbench/2023-12/dc0ba053-a1f0-4e6a-a5f8-e7668ddd2249/NCRB_STATS.pdf

[24] United Nations, Department of Economic and Social Affairs, Population Division. (2022). *World population prospects 2022: Summary of results*. United Nations. Retrieved from <https://population.un.org/wpp/>

[25] United Nations Office on Drugs and Crime. (2020, June 25). *UNODC World Drug Report 2020: Global drug use rising; while COVID-19 has far reaching impact on global drug markets*. Retrieved from <https://www.unodc.org/unodc/frontpage/2020/June/unodc-world-drug-report-2020-global-drug-use-rising-while-covid-19-has-far-reaching-impact-on-global-drug-markets.html>

[26] Singh, A. P., Seth, M., Bakshi, K., Uniyal, A. K., & Singh, H. (2023). JUVENILE JUSTICE IN INDIA—THE CHANGING FACE OF CRIMES BY YOUTH. *Russian Law Journal*, 11(5S), 156-161.

[27] Ministry of Law and Justice, Government of India. (2023). *Annual reports*. Department of Justice, Government of India. Retrieved from <https://doj.gov.in/annual-reports/>

[28] National Crime Records Bureau. (n.d.). National Crime Records Bureau (NCRB): Datasets. Data.gov.in. Retrieved October 25, 2025, from <https://www.data.gov.in/ministrydepartment/National%20Crime%20Records%20Bu>

reau%20(NCRB)

[29] Transparency International. (2022). *Corruption perception index 2022*. Retrieved from <https://www.transparency.org/en/publications/corruption-perception-index-2022>

[30] Central Vigilance Commission. (n.d.). Annual reports. Retrieved October 25, 2025, from <https://www.cvc.gov.in/annualreport.html>

[31] Vora, H. (2024). Police Brutality in India: Its Impact on Individuals and Their Rights. *LawFoyer Int'l J. Doctrinal Legal Rsch.*, 2, 306.

[32] Institute for Crime & Justice Policy Research. (n.d.). *World Prison Brief*. Retrieved October 25, 2025, from <https://www.prisonstudies.org/>

[33] Bureau of Justice Statistics. (n.d.). Recidivism and reentry. Office of Justice Programs. Retrieved October 25, 2025, from <https://bjs.ojp.gov/topics/recidivism-and-reentry>

while simultaneously reducing the populations of correctable police officers P_c^0 and correctable judges J_c^0 . This reflects a more efficient correction mechanism, whereby individuals spend shorter durations in correctable states before transitioning into stable, honest institutional roles. Moreover, the criminal compartments remain identically zero ($E^0 = C^0 = C_v^0 = 0$) for all values of k_2 , confirming the persistence of the crime-free equilibrium under enhanced judicial correction. Overall, these results highlight the critical role of judicial efficiency in shaping the institutional composition of the crime-free equilibrium. An optimized judicial correction rate k_2 promotes long-term crime prevention by strengthening honest institutional structures and accelerating transitions out of correctional states.

B Effect of Judicial Feedback Rate r_1 on Crime free equilibrium Point

Figure 4 illustrates the influence of the judicial feedback rate r_1 on the crime-free equilibrium structure as the total population N varies. The parameter r_1 represents the effectiveness of judicial rehabilitation and feedback mechanisms that promote lawful behaviour. As observed in Figure 4, increasing r_1 leads to a systematic increase in the susceptible population S^0 , indicating enhanced reintegration of individuals into lawful social states. This positive effect is accompanied by corresponding growth in the habitual police (P_h^0) and habitual judge (J_h^0) compartments, reflecting strengthened institutional stability under higher judicial feedback. Conversely, higher values of r_1 significantly reduce the equilibrium sizes of the correctable police (P_c^0) and correctable judges (J_c^0) compartments. This reduction suggests shorter durations in corrective or transitional judicial states due to more efficient rehabilitation and judicial outreach. Throughout all variations of r_1 , the criminal compartments remain identically zero, confirming the persistence of the crime-free equilibrium. Overall, these results demonstrate that stronger judicial feedback mechanisms substantially enhance equilibrium stability by reinforcing lawful

Appendices

A Impact of the judicial correction rate k_2 on Crime free Equilibrium Point

To examine the influence of judicial efficiency on the crime-free equilibrium, we analyzed the variation of equilibrium compartment values with respect to the total population size N for different values of the judicial correction rate k_2 , while keeping all other parameters fixed. The parameter values used were $\mu = 0.02$, $a_1 = 0.03$, $a_2 = 0.04$, $\eta_1 = 0.01$, $r_1 = 0.05$, and $\kappa_1 = 0.06$. As shown in Figure 3, all non-criminal equilibrium components scale linearly with the total population N , which is consistent with the structure of the crime-free steady state. The susceptible population S^0 remains unaffected by variations in k_2 , indicating robustness of the susceptible class under crime-free conditions.

In contrast, the redistribution among institutional compartments is strongly affected by k_2 . Specifically, increasing k_2 leads to higher equilibrium levels of habitual police officers P_h^0 and habitual judges J_h^0 ,

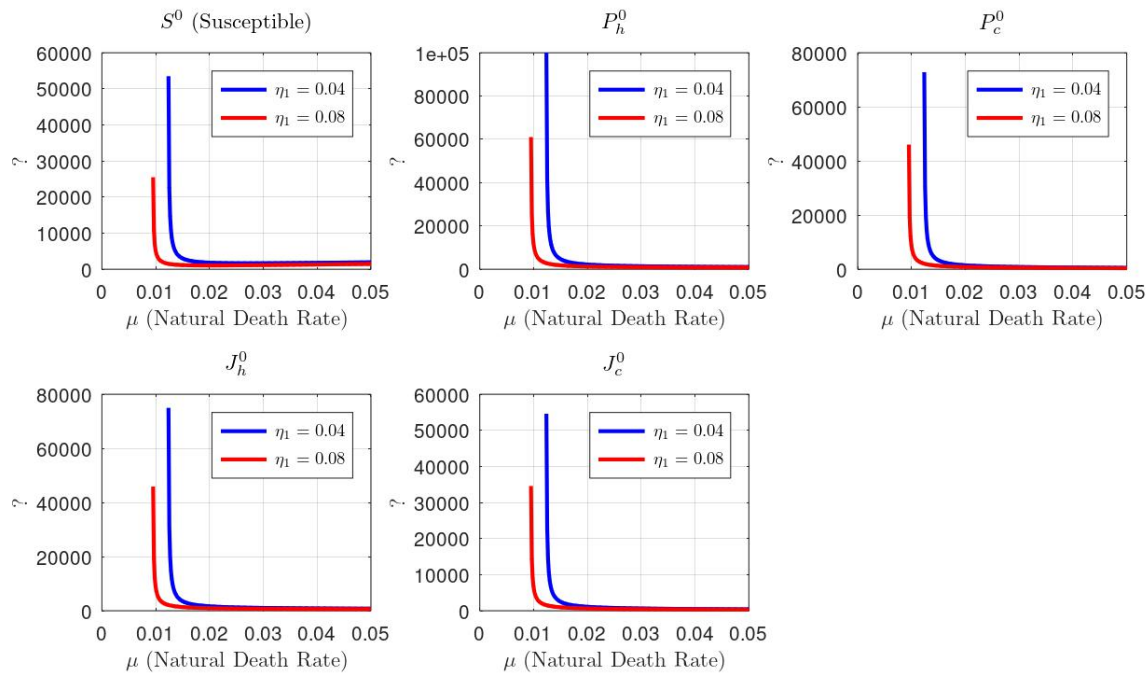


Figure A1. Impact of the natural death rate $\mu \in [0.005, 0.05]$ on the crime-free equilibrium variables S^0 , P_h^0 , P_c^0 , J_h^0 , and J_c^0 for two susceptibility rates $\eta_1 = 0.04$ (blue curves) and $\eta_1 = 0.08$ (red curves). All remaining parameters are fixed as $a_1 = 0.03$, $a_2 = 0.04$, $r_1 = 0.05$, $\kappa_1 = 0.06$, $\kappa_2 = 0.07$, and $N = 5000$. The plots demonstrate a strong inverse dependence of equilibrium populations on μ , with heightened sensitivity at lower μ values and systematically lower equilibria under higher susceptibility.

behaviour, reducing reliance on correctional structures, and suppressing the long-term potential for criminal resurgence. This highlights the critical policy role of judicial efficiency and rehabilitation programs in sustaining crime-free societal states.

C Impact of Natural Death Rate μ under Different Susceptibility Levels on Crime free Equilibrium Point

Figure A1 illustrates the variation of the crime-free equilibrium components S^0 , P_h^0 , P_c^0 , J_h^0 , and J_c^0 with respect to the natural death rate $\mu \in [0.005, 0.05]$ for two susceptibility levels $\eta_1 = 0.04$ and $\eta_1 = 0.08$. All equilibrium variables exhibit a pronounced inverse dependence on μ , with sharp declines observed at lower values of μ , indicating high sensitivity of the system in low-mortality regimes. As μ increases beyond approximately 0.015, the equilibrium values stabilize and approach near-zero levels, reflecting reduced population persistence in the crime-free state. Moreover, higher susceptibility ($\eta_1 = 0.08$)

consistently produces lower equilibrium populations across all compartments compared to $\eta_1 = 0.04$, demonstrating that increased exposure to criminal influence suppresses both susceptible and institutional populations at equilibrium. These results highlight the delicate balance between demographic attrition and crime vulnerability, suggesting that effective crime-prevention and public policy strategies must jointly address mortality effects and susceptibility reduction to sustain long-term social stability and institutional integrity.

Professor (Dr.) Ajay Ranga is serving as the Registrar at J.C. Bose University of Science and Technology, YMCA, Faridabad, and as Professor at the University Institute of Legal Studies (UILS), Panjab University, Chandigarh. He has previously served as Registrar (O), Finance Officer (O), Director of the Centre for Criminology and Forensic Science at Himachal Pradesh National Law University, Shimla, and Dean of Chitkara Law School, Chitkara University, Punjab.

He holds B.A. (Law), LL.B., LL.M., UGC-NET, and Ph.D. degrees. He has presented ninety-eight research papers in international, national, and regional conferences, and has published forty-four

research papers in reputed journals and edited volumes. He has authored two books: Crime Escalation and Slum Development and Role of Election Commission in India: Issues and Challenges. Professor Ranga has supervised numerous Ph.D. and LL.M. scholars and delivered invited lectures on prestigious platforms. He has served as Member Syndicate, Academic Council, Board of Finance, and as a Fellow (Senator) of Panjab University, Chandigarh. He has served on multiple academic and governmental committees, including the Bar Council of India, selection committees for faculty recruitment, and advisory boards of various journals. He is also the State President (Chandigarh) of the Drop Roball Federation India and the Kalaripayattu Federation of India. (Email: rangajay007@gmail.com, ajayranga@pu.ac.in)

Dr. Sarita Pippal is an Assistant Professor in the Department of Mathematics, Panjab University, Chandigarh, where she has been working since 2014 after previously serving at Ramjas College, University of Delhi. Her research interests include heat and mass transfer, fluid dynamics, fractional calculus, and mathematical modeling of natural and mixed convection phenomena. She has published several research papers in reputed international journals such as the International Journal of Heat and Mass Transfer and Contemporary Mathematics. She has presented her work at numerous national and international conferences and has delivered invited talks, supervised doctoral research, and participated in various faculty development programs and workshops. (Email: saritamath@pu.ac.in)